



2014-06

Development of carbon nanotube-based sensor to monitor crack growth in cracked aluminum structures underneath composite patching



Calhoun is a project of the Dudley Knox Library at NPS, furthering the precepts and goals of open government and government transparency. All information contained herein has been approved for release by the NPS Public Affairs Officer.

**Dudley Knox Library / Naval Postgraduate School
411 Dyer Road / 1 University Circle
Monterey, California USA 93943**



**NAVAL
POSTGRADUATE
SCHOOL**

MONTEREY, CALIFORNIA

THESIS

**DEVELOPMENT OF CARBON NANOTUBE-BASED SENSOR
TO MONITOR CRACK GROWTH IN CRACKED ALUMINUM
STRUCTURES UNDERNEATH COMPOSITE PATCHING**

by

Timothy M. Olson

June 2014

Thesis Advisor:
Second Reader

Young W. Kwon
Jarema M. Didoszak

Approved for public release; distribution is unlimited

THIS PAGE INTENTIONALLY LEFT BLANK

REPORT DOCUMENTATION PAGE			<i>Form Approved OMB No. 0704-0188</i>	
Public reporting burden for this collection of information is estimated to average 1 hour per response, including the time for reviewing instruction, searching existing data sources, gathering and maintaining the data needed, and completing and reviewing the collection of information. Send comments regarding this burden estimate or any other aspect of this collection of information, including suggestions for reducing this burden, to Washington headquarters Services, Directorate for Information Operations and Reports, 1215 Jefferson Davis Highway, Suite 1204, Arlington, VA 22202-4302, and to the Office of Management and Budget, Paperwork Reduction Project (0704-0188) Washington DC 20503.				
1. AGENCY USE ONLY (Leave blank)		2. REPORT DATE June 2014	3. REPORT TYPE AND DATES COVERED Master's Thesis	
4. TITLE AND SUBTITLE DEVELOPMENT OF CARBON NANOTUBE-BASED SENSOR TO MONITOR CRACK GROWTH IN CRACKED ALUMINUM STRUCTURES UNDERNEATH COMPOSITE PATCHING			5. FUNDING NUMBERS	
6. AUTHOR(S) Timothy M. Olson				
7. PERFORMING ORGANIZATION NAME(S) AND ADDRESS(ES) Naval Postgraduate School Monterey, CA 93943-5000			8. PERFORMING ORGANIZATION REPORT NUMBER	
9. SPONSORING /MONITORING AGENCY NAME(S) AND ADDRESS(ES) N/A			10. SPONSORING/MONITORING AGENCY REPORT NUMBER	
11. SUPPLEMENTARY NOTES The views expressed in this thesis are those of the author and do not reflect the official policy or position of the Department of Defense or the U.S. Government. IRB Protocol number ____N/A____.				
12a. DISTRIBUTION / AVAILABILITY STATEMENT Approved for public release; distribution is unlimited			12b. DISTRIBUTION CODE	
13. ABSTRACT (maximum 200 words) This paper presents the design of a carbon nanotube-based sensor to detect crack propagation in aluminum structures underneath composite patching. Initial tests are utilized to determine the correct procedure and materials to properly fabricate a carbon nanotube (CNT) sensor, which is then placed in between a composite patch and the aluminum structure. CNTs have been utilized as sensors in previous studies but only for sensing crack propagation within the composite itself. This study focuses on crack propagation in the base material and is not concerned with the composite. In this application, the composite is only a patch and can be replaced if damaged. This study utilizes both tension and fatigue testing to determine the usefulness of the CNT sensor. The CNT sensor is shown to be effective in giving an indication of the crack propagation in the aluminum. Correlation is done between the propagation length and the increase in resistance in the CNT sensor for tensile testing as the crack width is large enough to obtain an appreciable resistance change.				
14. SUBJECT TERMS CNT, sensor, crack propagation, tension and fatigue testing, resistance, aluminum.			15. NUMBER OF PAGES 81	
			16. PRICE CODE	
17. SECURITY CLASSIFICATION OF REPORT Unclassified	18. SECURITY CLASSIFICATION OF THIS PAGE Unclassified	19. SECURITY CLASSIFICATION OF ABSTRACT Unclassified	20. LIMITATION OF ABSTRACT UU	

THIS PAGE INTENTIONALLY LEFT BLANK

Approved for public release; distribution is unlimited

**DEVELOPMENT OF CARBON NANOTUBE-BASED SENSOR TO MONITOR
CRACK GROWTH IN CRACKED ALUMINUM STRUCTURES UNDERNEATH
COMPOSITE PATCHING**

Timothy M. Olson
Lieutenant, United States Navy
B.S., United States Naval Academy, 2009

Submitted in partial fulfillment of the
requirements for the degree of

MASTER OF SCIENCE IN MECHANICAL ENGINEERING

from the

**NAVAL POSTGRADUATE SCHOOL
June 2014**

Author: Timothy M. Olson

Approved by: Young W. Kwon
Thesis Advisor

Jarema M. Didoszak
Second Reader

Knox T. Millsaps
Chair, Department of Mechanical and Aerospace Engineering

THIS PAGE INTENTIONALLY LEFT BLANK

ABSTRACT

This paper presents the design of a carbon nanotube-based sensor to detect crack propagation in aluminum structures underneath composite patching. Initial tests are utilized to determine the correct procedure and materials to properly fabricate a carbon nanotube (CNT) sensor, which is then placed in between a composite patch and the aluminum structure. CNTs have been utilized as sensors in previous studies but only for sensing crack propagation within the composite itself. This study focuses on crack propagation in the base material and is not concerned with the composite. In this application, the composite is only a patch and can be replaced if damaged.

This study utilizes both tension and fatigue testing to determine the usefulness of the CNT sensor. The CNT sensor is shown to be effective in giving an indication of the crack propagation in the aluminum. Correlation is done between the propagation length and the increase in resistance in the CNT sensor for tensile testing as the crack width is large enough to obtain an appreciable resistance change.

THIS PAGE INTENTIONALLY LEFT BLANK

TABLE OF CONTENTS

I.	INTRODUCTION AND BACKGROUND	1
	A. COMPOSITE PATCHING.....	1
	B. NANOPARTICLES.....	1
	C. BENEFIT OF STUDY	2
	D. OBJECTIVES	4
II.	EXPERIMENTAL	5
	A. PROVING CONCEPT	5
	1. Nanoparticle Resistivity.....	5
	2. Resistivity of Laminating Resin with CNTs	6
	B. SAMPLE SPECIFICATION	8
	1. Sample Selection.....	8
	2. Sample Preparation	10
	3. Materials	11
	<i>a. Resin and Hardener</i>	<i>11</i>
	<i>b. E-Glass</i>	<i>12</i>
	<i>c. CNTs</i>	<i>12</i>
	<i>d. Tools / Equipment</i>	<i>13</i>
	4. Construction Technique/Procedure	13
	<i>a. Aluminum.....</i>	<i>14</i>
	<i>b. Bonding Agent.....</i>	<i>14</i>
	<i>c. Resin</i>	<i>14</i>
	<i>d. CNTs.....</i>	<i>14</i>
	<i>e. E-Glass</i>	<i>15</i>
	<i>f. Create Composite</i>	<i>15</i>
	<i>g. Vacuum Seal Composite</i>	<i>15</i>
	C. TENSILE TESTING	15
	D. FATIGUE TESTING.....	17
III.	RESULTS	19
	A. TENSILE TESTING	19
	1. Bare Aluminum.....	19
	2. Composite	20
	3. Composite with CNT Sensor.....	23
	B. FATIGUE TESTING.....	29
	1. Bare Aluminum.....	30
	2. Composite	30
	3. Composite with CNT Sensor.....	35
IV.	CONCLUSION	43
	A. DELAMINATION	43
	B. RESISTANCE.....	43
	C. USEFULNESS.....	43

APPENDIX A	45
A. INITIAL SAMPLE PREPARATION	45
B. MATERIALS/EQUIPMENT	45
C. CONSTRUCTION TECHNIQUE/PROCEDURE	46
1. Initial	46
<i>a. Aluminum</i>	<i>46</i>
<i>b. Bonding Agent</i>	<i>46</i>
<i>c. Resin</i>	<i>46</i>
<i>d. CNTs</i>	<i>47</i>
<i>e. E-Glass</i>	<i>47</i>
<i>f. Create Composite</i>	<i>47</i>
<i>g. Vacuum Seal Composite</i>	<i>47</i>
2. Final Changes	47
<i>a. Sample Size</i>	<i>47</i>
<i>b. Notch</i>	<i>48</i>
<i>c. Bonding Agent</i>	<i>48</i>
<i>d. Curing Time</i>	<i>49</i>
APPENDIX B	51
A. INITIAL TESTING	51
1. Eight-Inch Samples	51
2. Twelve-Inch Samples	56
LIST OF REFERENCES	59
INITIAL DISTRIBUTION LIST	63

LIST OF FIGURES

Figure 1.	CNTs formed in a line two inches in length (top to bottom).....	5
Figure 2.	CNT resin with increasing wt% of CNT from right (1%) to left (5%).....	8
Figure 3.	Bare aluminum sample with 3 inch width, warping can be seen on left side....	9
Figure 4.	Diagram of tension force and bending moment on sample (loading in Instron and MTS, left side, and resulting forces, right side).....	10
Figure 5.	Diagram with measurements of final sample design with “crack.” Measurements are in inches	11
Figure 6.	Picture showing location of loading grips and offset of sample to obtain a bending moment.....	16
Figure 7.	Loading curves for bare aluminum samples	20
Figure 8.	Loading curves for composite samples.....	21
Figure 9.	Delamination at the end of sample 4.....	21
Figure 10.	Delamination of sample 5 as loading is increased (left to right)	22
Figure 11.	Side view of sample 5 showing delamination location.....	22
Figure 12.	Side view of sample 5 showing delamination in composite.....	23
Figure 13.	Loading curves for CNT samples	24
Figure 14.	Side view of CNT sample 5 showing cracking in resin base layer next to composite	24
Figure 15.	Delamination of sample 5 containing CNTs as loading is increased (left to right).....	25
Figure 16.	Side view of CNT sample 5 showing small delamination in composite	25
Figure 17.	Defoprmtion for composite sample with CNT’s on top as top square.....	27
Figure 18.	Deformation for composite sample.....	28
Figure 19.	Tensile loading resistance graph.....	29
Figure 20.	End view of bare aluminum showing fracture surface	30
Figure 21.	Delamination of sample 1 during loading from no load (left) to aluminum has fully fractured (right)	32
Figure 22.	Sample 4 showing delamination within the composite only	33
Figure 23.	Sample 4 showing no delamination between layers or aluminum.....	33
Figure 24.	Growth of crack in aluminum for composite sample 1 from no cycles (top left) to under ¼ inch (top right) to ½ inch (bottom left) to complete failure (bottom right)	34
Figure 25.	Cracked edge of sample 2 showing brittle fracture surface.....	35
Figure 26.	Delamination of sample 2 during loading from no load (left) to aluminum almost fully fractured (right).....	36
Figure 27.	Sample 2 showing delamination within the composite only	37
Figure 28.	Sample 2 showing no delamination between layers or aluminum.....	37
Figure 29.	Growth of crack in aluminum for CNT sample 2 from no cycles (top left) to under ¼ inch (top right) to ½ inch (bottom left) to complete failure (bottom right)	38
Figure 30.	Cracked edge of sample 2 showing brittle fracture surface.....	38

Figure 31.	Graphical comparison between bare aluminum, composite and CNT cycles to failure	40
Figure 32.	Cyclic fatigue resistance change for each sample.....	41
Figure 33.	Diagram with measurements of initial sample design with notch, measurements are in inches	45
Figure 34.	Bare aluminum sample with 3-inch width, warping can be seen on left side..	51
Figure 35.	CNT sensor utilization and proof of usability.....	52
Figure 36.	Eight inch samples, before testing (left), initial delamination (middle), final catastrophic delamination (right).....	53
Figure 37.	Delamination occurring between the base resin layer and the composite	53
Figure 38.	Full length composite sample, initially unloaded (left), initial delamination (middle), final delamination (right)	54
Figure 39.	Full length composite sample showing delamination between the base resin layer and the composite.....	54
Figure 40.	Full length composite sample with CNT sensor, initially unloaded (left), initial delamination (middle), final delamination (right)	55
Figure 41.	Full length composite with CNT sensor showing delamination between both base resin layer and aluminum (middle) and base resin layer and composite (right).....	55
Figure 42.	12 inch sample showing delamination progression around pre crack area from left to right.....	56
Figure 43.	Delamination between the base resin layer and the composite around the crack area	56

LIST OF TABLES

Table 1.	CNT resistance.....	6
Table 2.	Resistance of laminating resin with CNTs.....	7
Table 3.	Loading difference between sample location	17
Table 4.	Breakdown comparison of loading for each set of samples	26
Table 5.	Thickness of composite and CNT samples.....	26
Table 6.	Resistance increase per crack length.....	29
Table 7.	Bare aluminum cycles to failure	30
Table 8.	Composite cycles to failure.....	31
Table 9.	CNT cycles to failure	36
Table 10.	Numerical comparison between bare aluminum, composite and CNT cycles to failure	39

THIS PAGE INTENTIONALLY LEFT BLANK

LIST OF ACRONYMS AND ABBREVIATIONS

CNT	carbon nanotube
MWCNT	multi-walled carbon nanotube
SWCNT	single-walled carbon nanotube
DWCNT	double-walled carbon nanotube
Wt%	weight percent
SD	standard deviation
ASTM	American Society for Testing and Materials

THIS PAGE INTENTIONALLY LEFT BLANK

ACKNOWLEDGMENTS

I would like to thank Professor Kwon for all of the assistance and guidance given throughout this study.

I would also like to thank Jake for his teaching and review.

THIS PAGE INTENTIONALLY LEFT BLANK

I. INTRODUCTION AND BACKGROUND

A. COMPOSITE PATCHING

The superstructure of Ticonderoga class cruisers is constructed from aluminum alloy 5456. It has been determined that the aluminum alloy becomes sensitized at elevated temperatures due to incorrect processing (heat treatment) in the creation of the aluminum alloy. Under loading the result of this “sensitization” is cracking in the aluminum [1, 2]. Completely removing the cracked sections of the superstructure and replacing it with new aluminum is problematic and eliminates this as a viable repair plan. Instead, utilizing polymer composite materials, a composite patch is created and placed over the cracked aluminum. The composite patch maintains the integrity of the aluminum structure due to the filling of the crack and sharing the applied load with the cracked aluminum structure. Composites have been utilized in other countries for years, dating back as early as the 1950s [1]. It has been only in the last 30 years that the United States has started to develop composites in full scale ship hull or superstructure construction [1–3].

B. NANOPARTICLES

Nanoparticles are simply particles of nanometer size and can be created from many different materials. Carbon nanotubes (CNTs) are by definition carbon tubes where the diameter of the tube is nanometers in size. The CNTs by themselves have great strength, stiffness and are relatively ductile, and according to Calliser, “is the strongest known material” [2]. With these highly desirable qualities, CNTs have been added to other materials to increase its overall strength like composites. A technical report published by Ahwahnee Technology describes that approximately one weight percent of CNTs is enough to obtain “appreciable” increases in strengthening properties “like fracture toughness” of thermo-set plastics like resin which is utilized in composites [3]. Other research has shown that as little as 0.1 weight percent is large enough to provide increases in strength and Young’s modulus [4].

There are three typical types of carbon nanotubes consisting of single-walled, double-walled, and multi-walled. It is important to note that multi-walled carbon nanotubes were utilized for this study. Multi-walled carbon nanotubes (MWCNTs) are single-walled carbon nanotubes (SWCNTs) wrapped inside one another like a shell. Double-walled carbon nanotubes (DWCNTs) simply have two layers; while MWCNTs have more layers [5, 6]. For ease of understanding, all CNT's referred to within this study are to be considered MWCNTs. The experimentation conducted here can be done with SWCNTs, but due to supply, MWCNTs were employed. By physical observation, the MWCNTs act like SWCNTs as only the outer shell of the MWCNTs are able to be observed [6]. It has also been shown from research at the Naval Postgraduate School (NPS) that CNT's have electrical conductive properties by themselves, and maintain a certain amount of conductivity when mixed with resin [7]. Bily applied CNTs to the middle layer of a carbon fiber composite, which has an initial interlayer crack. The resistance increase was recorded when the interface crack propagated in the samples under Mode II fracture testing [5]. It has been shown in many studies that the addition of CNTs to composites increases their overall strength [5, 6, 10, 11, 12, 13, 14].

Gao et al. completed a study of uniform and non-uniform dispersed carbon nanotubes. They concluded that resistance in the CNTs increased when placed under cyclic fatigue [8]. Low concentrations of CNTs appeared to be ineffective in conduction but larger amounts proved useful [11, 12, 13, 14, 16, 17, 18]. No specific weight percent of CNTs have been described as the best as it is generally dependent on the application. The specific weight percent utilized in this study can be seen in the Experimentation section.

C. BENEFIT OF STUDY

The high cost of removing and replacing cracked pieces of the superstructure of Ticonderoga class cruisers forces the Department of Defense and the Navy to find alternative ways of repairing the cracks. As previously stated, the current method used for repair is placing a composite patch over the crack in order to redistribute the stress around the crack and through the composite. Along with cost, in situ repair is a major

benefit of composites as compared to full removal of the damaged material. However, once a composite patch is applied, it is unknown whether the crack is propagating under the composite as paint is typically placed over the composite. The idea of placing strain gauges at the site of the crack to track any propagation is too costly and would create an impurity around the location. This study focuses on employing CNTs to develop a sensor that will incorporate a mixture of resin and CNTs, which will be homogeneous in nature to the composite patch. Exploiting the electro conductivity of the sensor, the crack propagation of the base structure will be determined. This study will utilize both tensile and fatigue testing of the sensor, but it will not be using aluminum alloy 5456. A lower strength aluminum alloy is used in order to complete testing on the available laboratory instruments. However, upon completion of testing this sensor will be able to be utilized for any base material, not solely aluminum.

Unlike previous studies, this study is primarily concerned with the crack propagation in the base material which is different from the composite patch. Though it uses only aluminum as the base material, it is applicable to all metals. Most research completed has been focused on the composite structure and the interaction with the composite only [4, 9, 10, 11, 12]. From previous studies, it has been found that the CNTs can act as a sensor within composites [11, 13, 14, 15]. The purpose of this study is to determine whether the increase in resistance in the CNTs from tensioning and cyclic loading of the composite/aluminum structure can be utilized to identify if the aluminum is failing and, specifically, in this case, continuing to crack. A key difference from previous studies is that the CNTs will not be dispersed within the resin used in the creation of the composite. By having the CNTs in a specific location, like at the tip of the crack, it will only detect if the crack is propagating. There is little concern about damage in the composite as it can be easily removed and replaced. Having only a small piece of CNTs reduces the cost in CNTs, as only a small amount is needed to create the sensor. It also reduces the process in creating the composite structure by not including the CNTs within the composite. Some may say that small sensors already exist and can be utilized instead of using the CNTs to detect crack propagation. Small special-use sensors have been created from copper to detect crack propagation in a base material [16]. They are

small and accurate, yet that accuracy and size introduces a large price. In the current defense budget, low-cost applications are necessary.

The development of this sensor will allow personnel to determine whether the patch is effective and provide long-term testing in the life expectancy of the patches. These sensors are also of a homogeneous nature of the composite patch itself, as the same resin is utilized in creating the sensor. This study will provide a possible avenue for the Navy and Department of Defense to monitor the cracks over an extended period of time to better determine the future of the cruisers and other ships incorporating aluminum in its construction.

D. OBJECTIVES

1. To create a sensor made of CNT and resin
2. Fabricate samples utilizing the CNT sensor
3. Test samples and compare to bare aluminum, and composite samples

II. EXPERIMENTAL

A. PROVING CONCEPT

1. Nanoparticle Resistivity

As described earlier, carbon nanotubes (CNTs) have electrical characteristics which allow them to conduct electricity. Though not as conductive as 28 gauge steel galvanized wire (utilized in this study), which has a resistance of approximately 2Ω for a two inch sample, using two inch lengths as a comparison, CNTs have approximately $6k\Omega$'s of resistance. It is important to understand that this is measuring the resistance of CNTs on a flat surface spread out over a 2 inch distance. An individual CNT has a much lower resistance. In normal form, CNTs looks like black dust as shown in Figure 1. The dust is actually clumps of CNTs as the eye cannot see nanoparticles without some type of magnification. The clumps are due to Vander-Wall forces which will not be discussed in this study [3].



Figure 1. CNTs formed in a line two inches in length (top to bottom)

In order to measure the resistance between the two ends of CNTs, the current must travel through the CNTs. There must be a connection from one CNT to another,

and if there is air between them the path will change. There is a small amount of air all throughout the CNTs within the sample in nanometer scale. This air though small, forces the link between the two ends to be slightly longer than two inches. Though this is occurring on the nanometer level, it does affect the resistance as the distance traveled is longer or shorter depending on the exact path taken from one end to the other. This can be seen experimentally as the straight line distance between the two ends is 2 inches. Placing the electrical leads at different locations along the ends resulted in different resistance values varying the overall value by approximately 0.82kΩ for 10 samples as shown in Table 1. It is important to note the electrical leads utilized in the testing were both moved to ensure the straight line distance remained at 2 inches.

Table 1. CNT resistance

Resistance of 2-inch sample CNT										
Resistance ($k\Omega$)	6.00	5.90	6.00	6.20	6.00	6.40	7.70	5.40	7.20	4.60
Average ($k\Omega$)	6.14									
Standard Dev ($k\Omega$)	0.82									

The higher the resistance, the less conductive the material is. Thus, as compared to the steel wire, the CNTs are an order of magnitude less conductive. This is important as later in the study only approximately two inches of CNTs are used while 4-10 inches of steel wire is used to obtain the resistance through the CNTs. With the CNTs resistance in the thousands of ohms, adding less than 20 ohms from the wire is insignificant and the resistance recorded is considered that of the CNTs.

2. Resistivity of Laminating Resin with CNTs

The laminating resin by itself is nonconductive. The construction of the laminating resin includes resin and a hardener. By total volume and weight the ratio of resin to hardener is 100:33 and 100:30 respectively [17]. It is important to note that for the remainder of the study “resin” will be considered the correct mixture of resin and hardener already combined. After mixing and weighing the resin, different weight percent (wt%) amounts of CNTs were added to the resin ranging from 1 to 5 wt% of the

resin, as shown in Table 2. These were created and measured individually for each wt% of CNTs. The process operated by simply stirring in the CNTs into the resin. This is overly simplified as compared to a study by Sandler et al. They employed stirring machines rotating at 2,000 rpm. Due to the lack of equipment availability, stirring by hand was used in this study. It is important to note, though the resistance values found varied they were similar to those obtained in the study by Sander et al. They obtained resistance values in the range from 200 Ω to 20 M Ω which is comparable to the values shown in Table 2 [11].

Table 2. Resistance of laminating resin with CNTs

Resistance per wt%					
Weight % of CNT's	5	4	3	2	1
Sample 1 ($k\Omega$)	6.8	267	956	OVLD*	OVLD*
Sample 2 ($k\Omega$)	6.2	117	3600	OVLD*	OVLD*
Sample 3 ($k\Omega$)	8.2	148	1110	OVLD*	OVLD*

It was found that resistance increased as the wt% decreased from 5 to 1%. At 2 and 1 wt% the resistance was too large to record and an over load (OVLD*) was recorded. This occurs as there are not enough CNTs to carry the current because they are too spread out and the overall mixture becomes non-conductive. The CNTs are suspended in the resin and as the wt% decreases below a threshold of about 3 weight percent the CNTs are no longer forming a continuous line for the current to be carried through.

It was found by comparing the 5 wt% in Table 2 to the resistance recorded by the CNTs in air that they are close in value. Looking at the final cured product of the different samples shown in Figure 2 and the values recorded in Table 2, it is found that the 4 wt% of CNTs gives a good value for resistance and appears relatively consistent (not too viscous and has a good distribution of CNTs) as compared to straight resin without CNTs. The addition of CNTs to the resin causes the resin to thicken, thus reducing its viscosity. This is good as the less viscous the mixture is the less likely the CNTs will settle at the bottom of the mixture. This movement of the CNTs within the resin would decrease the uniform distribution of CNTs within the resin and result in an

unreliable resistance reading [7, 18]. This takes the optimal wt% of CNTs based on the samples resistance characteristics and visual appearance. In order to minimize the introduction of a defect in the overall composite patch design, it is important to maintain homogeneity of the base layer of resin and the CNT/resin mixture with that of the composite patch resin.

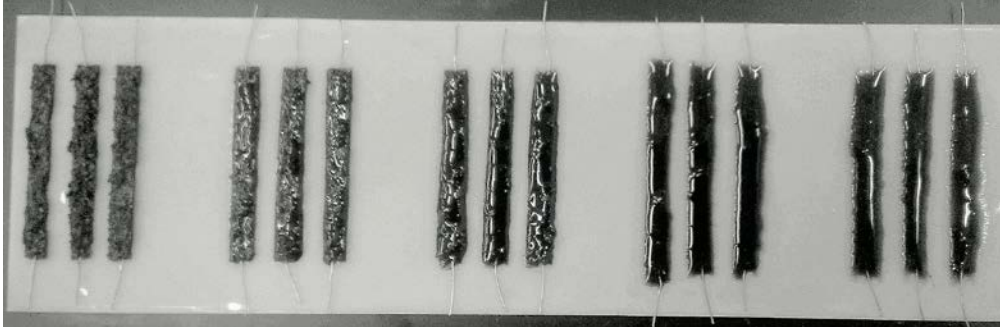


Figure 2. CNT resin with increasing wt% of CNT from right (1%) to left (5%)

B. SAMPLE SPECIFICATION

1. Sample Selection

The overall goal of this study is to determine whether CNTs can be employed to create a sensor to detect crack growth in the aluminum. From the introduction, it can be seen that sensors have already been created to detect crack growth in the composite. In order to change the desired location of crack monitoring from the composite to the base material a sample was created. The sample needed to show similar behavioral characteristics to the large structures of naval ships in order for the results to be directly applicable to the ships. This desire along with the capabilities of the laboratory equipment operating the Instron 4507 (tension instrument) and the MTS 858 table top system using the TestStarII program (fatigue instrument) gave initial sample size requirements [19, 20, 21]. If the sample was larger than 1 and ½ inches in width, bending would occur within the sample and would cause the sample to bow as shown in Figure 3.

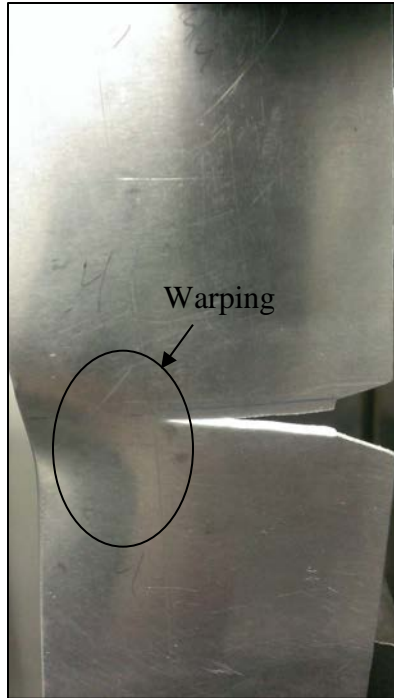


Figure 3. Bare aluminum sample with 3 inch width, warping can be seen on left side

This was an undesirable outcome as it would not be seen in the larger structures on ships, thus the maximum width was set as 1 and ½ inches. The desire to have the sample as wide as possible allows both bending moments and tension forces to occur thus increasing the stresses at the stress concentration location as shown in Figure 3. This ensures failure at an overall lower tensile load which was required for the MTS. The overall load required to propagate a crack in the sample needed to be small enough for the same sample design to be utilized in both instruments (Instron and MTS), and the MTS has a maximum loading of 10kN [20]. Additionally, such a loading as shown in Figure 4 would prevent the instantaneous crack growth leading to complete separation of the samples. In that situation, the CNT sensor does not serve the designed purpose.

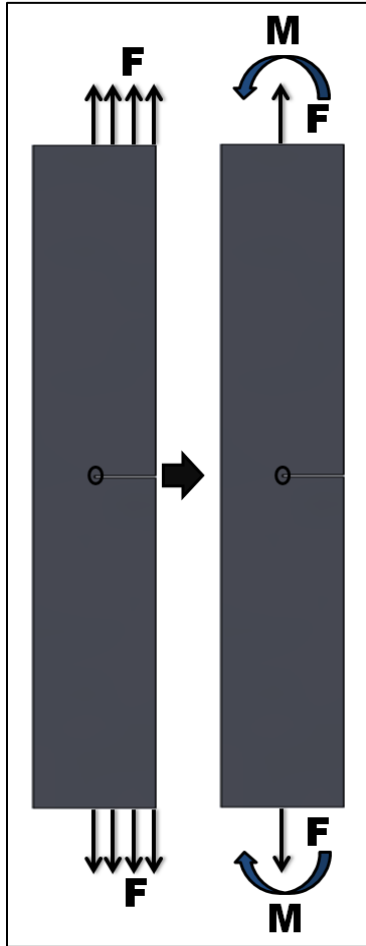


Figure 4. Diagram of tension force and bending moment on sample (loading in Instron and MTS, left side, and resulting forces, right side)

Initial experiments were completed utilizing specimens at 8 inches in length as described in Appendix A and shown in Appendix B. The results were not consistent with real world failure and thus the length was increased to 12 inches. The results obtained by these more closely matched what has been physically seen in the fleet. The bonding agent utilized changed through the study which also showed significant changes in the results which is described in Appendix A.

2. Sample Preparation

As stated within the introduction, the specific aluminum alloy utilized within the fleet is 5456. The aluminum alloy used for this study was 5086. It was selected based on

cost and its decreased strength for the limitations of the equipment utilized. Aluminum alloy 5086 was obtained in 12-inch square sheets with a thickness of 1/8th of an inch. Initial specimen fabrication is described in Appendix A. The final specimen dimensions are 12 inches in length and 1 and 1/2 inches in width. An initial “crack” or cut is utilized to facilitate a preexisting crack where the crack will propagate from as seen in Figure 5. The edge crack is located in the center of the sample along the length. The measurement of 5.98 inches shown in Figure 5 excludes half of the crack width, thus the crack is centered at 6 inches from the edges.

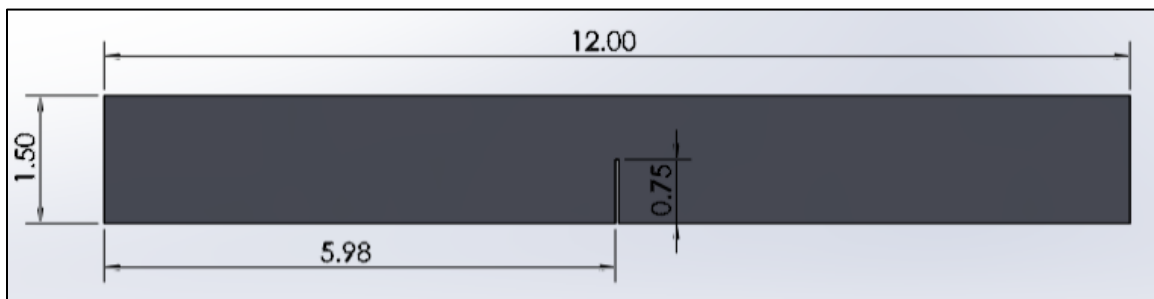


Figure 5. Diagram with measurements of final sample design with “crack.”
Measurements are in inches

3. Materials

a. *Resin and Hardener*

For this study M1002 resin was used with 226 and 237 hardeners made by Pro Set Inc. [17]. These are older versions of the current products being sold by Pro Set Inc. and are being utilized due to availability. The manufacturing and processing of the resin and hardeners have changed slightly, but the resin’s characteristics and strengths have not. The 226 hardener is considered a “medium laminating hardener” in reference to its pot life of 28 minutes [17]. The pot life refers to the length of time from mixing the resin and hardener together to initial set. The 226 hardener is utilized for making the CNT sensor component and for the base layer of resin initially placed on the sample. The 237 hardener is considered an “extra slow laminating hardener” in reference to its 80 minute pot life [17]. The 237 is utilized with the resin to laminate the E-Glass fibers. The longer

pot life allows many layers of E-Glass to be placed in location before the resin sets up. All samples were cured at room temperature and no heat was added post set up to reach final cure. The intent of the study is to determine if the sensor can be utilized to detect crack growth in the base material and decreasing the strength of the composite is not a deciding factor if it works or not. Also, the composites currently created for shipboard use are not heat treated after being applied, thus this study more closely mirrors the shipboard application.

b. E-Glass

For this study, 7500 Hexcel 6 ounce plain weave E-Glass fabric was selected. It has a nominal thickness of .0093 inches, and is considered a lightweight cloth employed commonly in small craft boat building [22]. Each layer of fabric is considered a ply, and the more plies used the thicker and stronger the overall composite will be. For this study seven plies were used. The amount of plies corresponds with the thickness and strength of the base material, and the composite needs to be thick enough to share enough load with the base material. The specific weave and size of E-Glass employed is in comparison with the size and strength of aluminum. As the fleet utilizes larger and thicker aluminum the weave is tighter and contains larger fibers. The plies were cut and placed in such a way that each subsequent layer was larger than the previous. This creates a stacking area which aids in distributing the load through the composite and ensures adhesion of each layer to the base layer of resin.

c. CNTs

As described previously the wt% of CNTs added to the resin changes its overall concentration and resistance values. After many test samples at various wt% of CNTs, 5 wt% was deemed to be optimal as it maintained an initial resistance below 300k Ω 's and ensured the initial mixture was thicker and would not run off the sample while the composite was applied. Testing and results at lower wt% of CNTs are provided in Appendix B.

d. Tools / Equipment

The tools and equipment utilized in order of use to create each sample include:

- Aluminum Sample (pre-fabricated with crack)
- Safety Goggles
- Power Sander utilizing 80 Grit Sand Paper
- Powder Free Latex Gloves
- DX-579 Metal Cleaner
- Lint Free Rags
- Distilled Water
- 3M Bonding Agent
- Mixing Buckets
- Cab-o-Sil Filler (thickener)
- 28 Gauge Steel Galvanized Wire
- CNTs
- Scale
- Scissors
- Teflon Sheets
- Fabric Cutting Wheel/Board with Ruler
- Nylon Peel Ply
- Perforated Release Film
- Bleeder Cloth
- Vacuum Bag
- Tacky tape
- Vacuum Pump with Gage
- Plastic Tubing

4. Construction Technique/Procedure

The following is the final procedure for creating the samples. This procedure changed through the study as better methods/materials were employed to improve the overall process and improve the final composite product with CNT sensor. The initial

procedure and the reasoning behind why parts/materials were changed are detailed in Appendix A.

a. Aluminum

- Cut out sample size of aluminum to desired width and length. (1 and ½ inches by 12 inches)
- Cut crack into sample to introduce stress concentration.
- Sand top side of sample to ensure entire surface is roughened.
- Clean metal surface with metal cleaning agent.

b. Bonding Agent

- Mix saline bonding agent parts a and b together, allow to sit for 30 minutes.
- Allow surface to dry from cleaning agent and apply water drop test (water does not bead) to ensure little to no surface tension in water. If test fails, repeat cleaning and test again.
- Apply saline bonding agent to surface and let sit for at least 1 minute.
- Remove excess saline bonding agent by dabbing a pre-wetted cloth with bonding agent. DO NOT RUB as described in directions on bottle for use.

c. Resin

- Mix resin and hardener as prescribed with thickener (cab-o-sil).
- Cover sample with a thin layer of epoxy and ensure crack is filled in. Let sit for at least 1 hour, but no longer than 3 hours. (Do not allow base layer to harden before applying CNT sensor or composite) Keeping the base layer tacky but not solid allows for best bonding and maintains homogeneity.
- Mix resin and hardener for CNT sensor.

d. CNTs

- Weigh mixed resin and add five wt% of CNT to resin.
- Place CNT resin on sample in front of notch point.
- Place 28 gauge wire in both ends of the CNT resin long enough to extend past the end of the sample.

e. E-Glass

- Cut set number of E-Glass fibers to needed size and shape.
- Mix resin and hardener for composite.

f. Create Composite

- Apply E-Glass fiber sheets and coat with resin ensuring even and full coating.
- Apply bleeder sheet to top of sample followed by cloth.

g. Vacuum Seal Composite

- Place seal over entire sample and vacuum out air to -10 mmHg and hold for 8 hours.
- Once hardened remove excess epoxy and test sample.

C. TENSILE TESTING

For the purpose of this study, total fracture of the specimen is not desired. Only crack initiation and propagation to a set point is required. Thus, the specimens were aligned in the Instron as shown in Figures 4 and 6 where the force would be applied as a tensile load on the right side (cut side) and compression load due to bending on the opposite side. This would allow the crack to initiate and begin to propagate, but not completely fracture the specimen as the stress within the sample would change from a larger tension to a smaller tension with the combined loads of the axial and bending. This would allow enough time to stop the test prior to complete fracture. The desire of this testing is showing the crack in the aluminum growing and the corresponding increase in resistance in the CNT sensor.

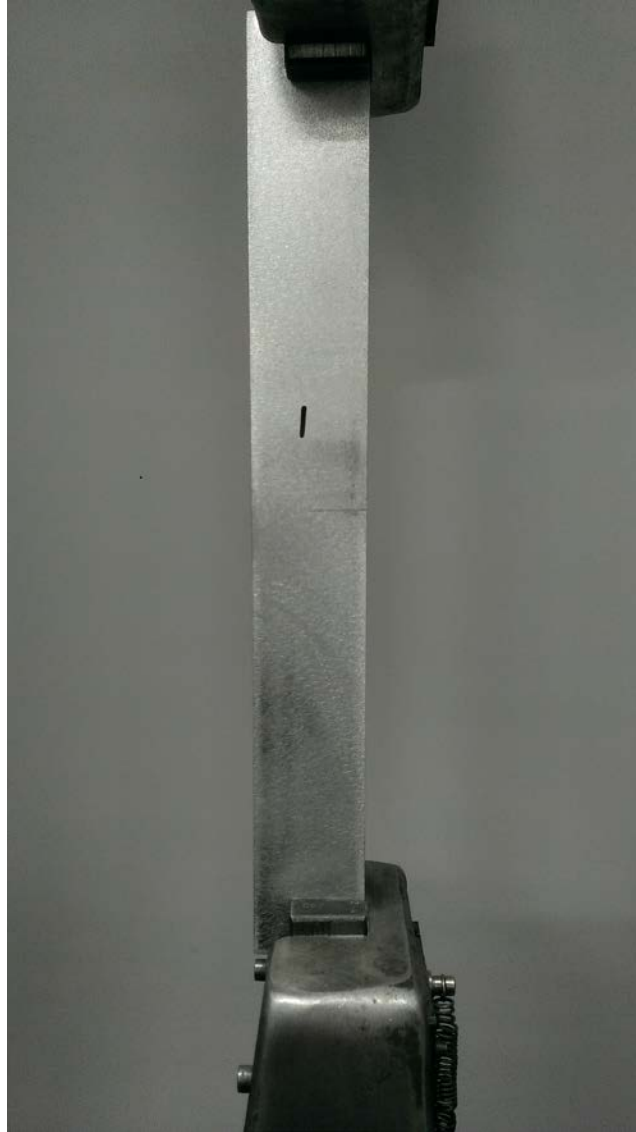


Figure 6. Picture showing location of loading grips and offset of sample to obtain a bending moment

Initial testing was completed to determine the differences between the loading as designed and normal central loading. As seen in Table 3, the crack would initiate at an average of 13.05kN and would propagate to failure more quickly for the center loading. The time to failure was approximately 80% less if the samples were placed centered in the Instron. A higher time to failure is desired as once the composite patch is placed over the crack a higher load will be required to initiate the crack. At that higher load the crack will propagate faster and the data recorded will be minimal. Thus, for this study the

lower the load to propagate the crack improves the accuracy of the data as more data will be able to be obtained. Centering the load on the right edge will increase the stress concentration at the crack tip and decrease the overall required load to initiate the crack.

Table 3. Loading difference between sample location

Sample location	Centered	Off center
Crack initiation (kN)	13.05	6.71
Time to propagate (s)	28.04	50.35

D. FATIGUE TESTING

For fatigue testing, the MTS used in this research has a maximum load of 10kN [20]. This is below the max load to initiate a crack in the centered method sample. From Table 3, the edge centered sample is found to have an average max load of 6.71kN to initiate a crack. This maximum is below the threshold of the instrument, thus the edge centered method was utilized with both instruments in order to obtain comparable data using the exact same method and sample preparation.

THIS PAGE INTENTIONALLY LEFT BLANK

III. RESULTS

A. TENSILE TESTING

All tensile testing utilized five samples of same design and composition. Three sets of samples (bare aluminum, composite, composite with CNT sensor) were created in order to show the difference between each.

1. Bare Aluminum

Figure 7 shows the loading versus displacement curves for 3 out of 5 samples tested with bare aluminum. Only three samples were used in the figure as the other two matched graphically but caused the figure to be overcrowded. Samples 1 and 2 did have a higher max loading which causes the average max loading line shown in Figure 7 to appear above the max loads displayed. The end of each curve is at the maximum load where the crack in the aluminum starts to propagate. The load decreases considerably after the crack initiates thus further loading is not shown.

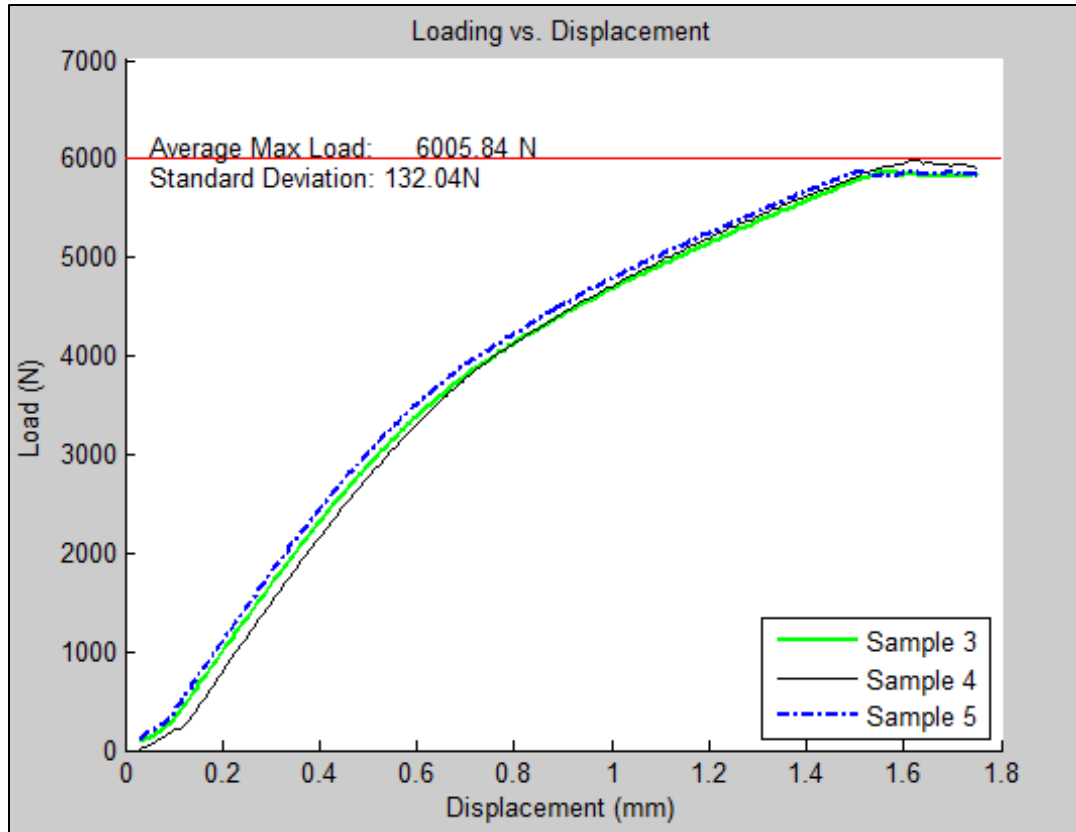


Figure 7. Loading curves for bare aluminum samples

2. Composite

Figure 8 shows the loading versus displacement curves for 3 out of 5 samples tested with a composite patch attached to the aluminum. Similar to Figure 7, only three out of five samples were graphed as samples 2 and 5 matched graphically but were removed to prevent overcrowding of the figure. Sharp drops in loading can be seen in each sample near higher loads. This is due to delamination occurring at the ends of the samples at this higher loading. The delamination occurs suddenly causing a rapid drop in loading as shown by the downward drop of sample 4 in Figure 8. Figure 9 shows an image of sample 4 at the end where the delamination occurred.

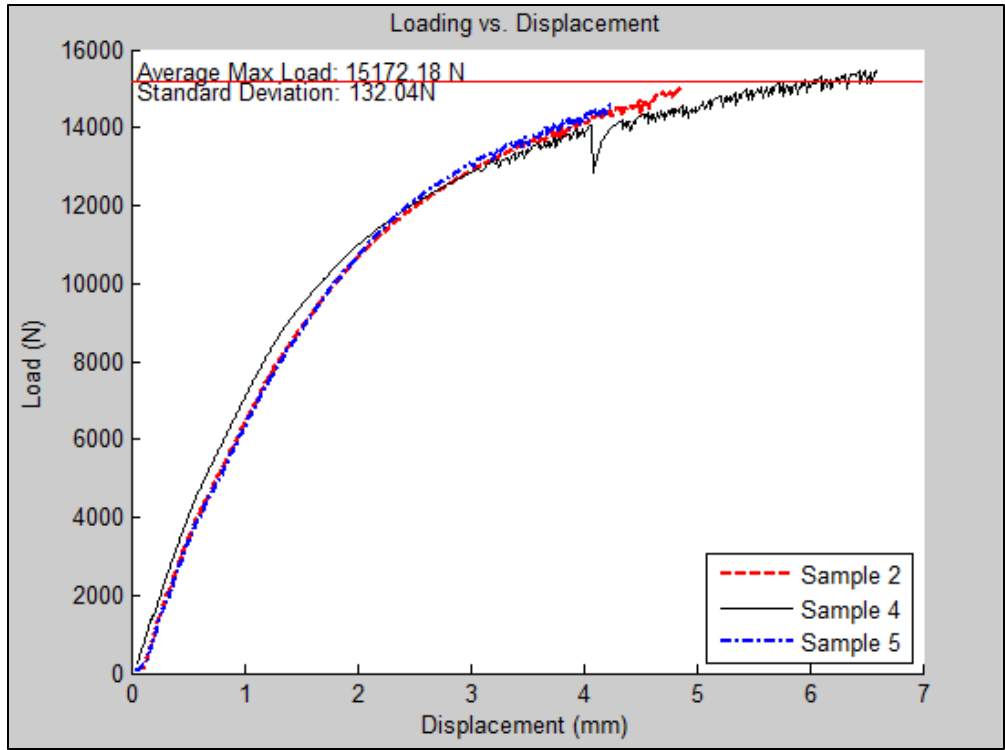


Figure 8. Loading curves for composite samples



Figure 9. Delamination at the end of sample 4

Figure 10 shows that the delamination in the center of sample 5 growing as the loading is increased to a maximum load of 14633.28N. The delamination is shown as the white areas as it is between the individual layers of the composite as shown in Figures 11 and 12.



Figure 10. Delamination of sample 5 as loading is increased (left to right)

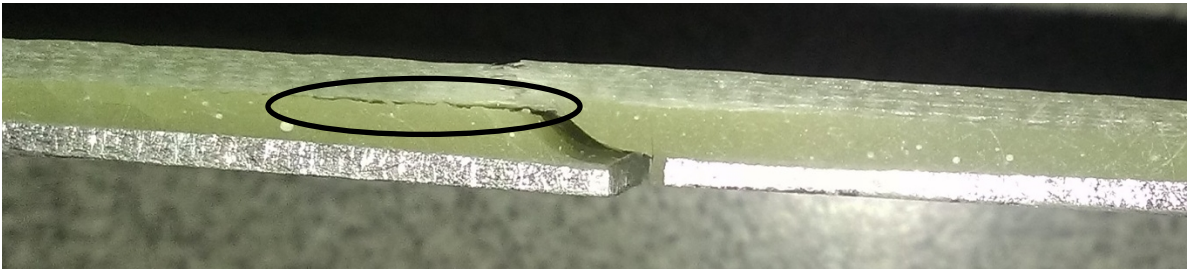


Figure 11. Side view of sample 5 showing delamination location

Figure 11 shows delamination between the composite and the base layer of resin along with the cracked base layer near the crack in the aluminum. But, delamination between the base layer and the aluminum has not occurred. Figure 12 shows the delamination within the composite from the side as the layers are white and slightly spread out.



Figure 12. Side view of sample 5 showing delamination in composite

3. Composite with CNT Sensor

Figure 13 shows the loading versus displacement curves for 3 out of 5 samples tested with CNTs added to the composite patch attached to the aluminum. Similar to Figures 7 and 8, only three out of five samples were graphed as samples 2 and 4 matched graphically but were removed to prevent overcrowding of the figure. Similar to the composite samples shown in Figure 8 sharp drops in loading occurred due to rapid delamination at either the edges or near the pre-crack of the samples. This did not affect the samples near the crack location as there was no delamination between the base resin layer and the aluminum as shown in Figure 14. Cracking did occur in the base resin layer but only where connected to the composite.

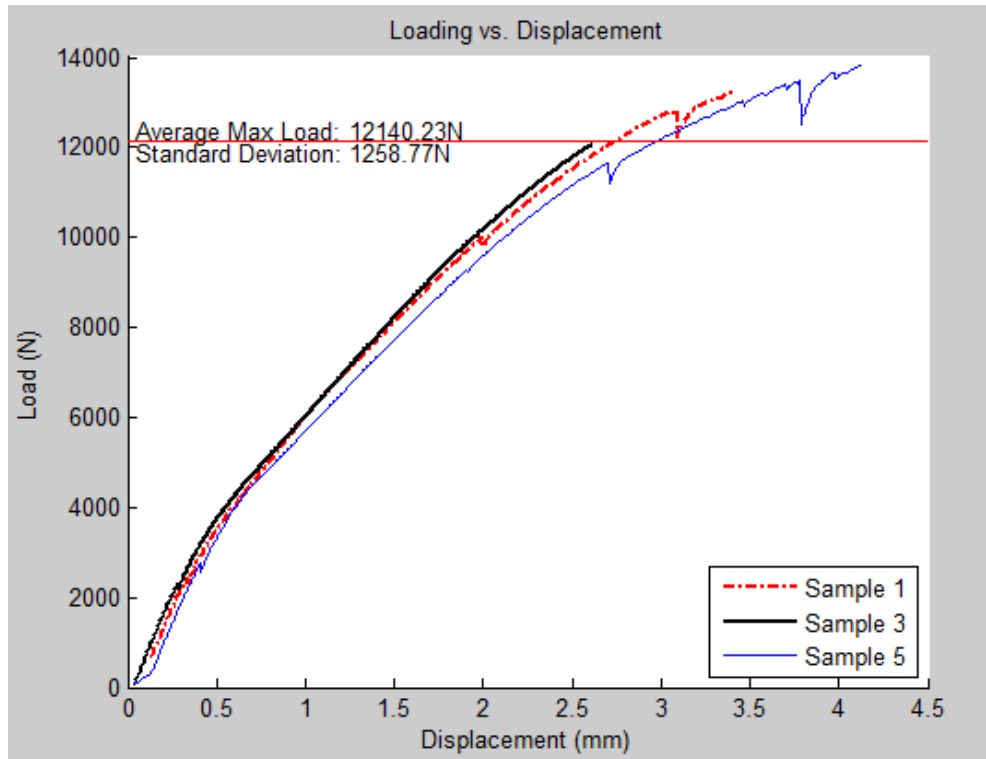


Figure 13. Loading curves for CNT samples

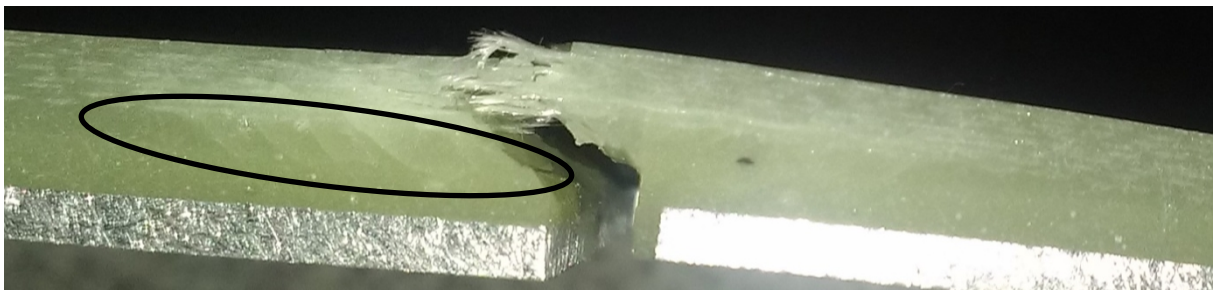


Figure 14. Side view of CNT sample 5 showing cracking in resin base layer next to composite

Figure 15 shows the delamination growth in sample 5 as the loading was increased to a max load of approximately 13,838N. Similar to Figure 10, delamination is shown as the white area within the sample. This delamination is within the composite itself as shown in Figure 16.

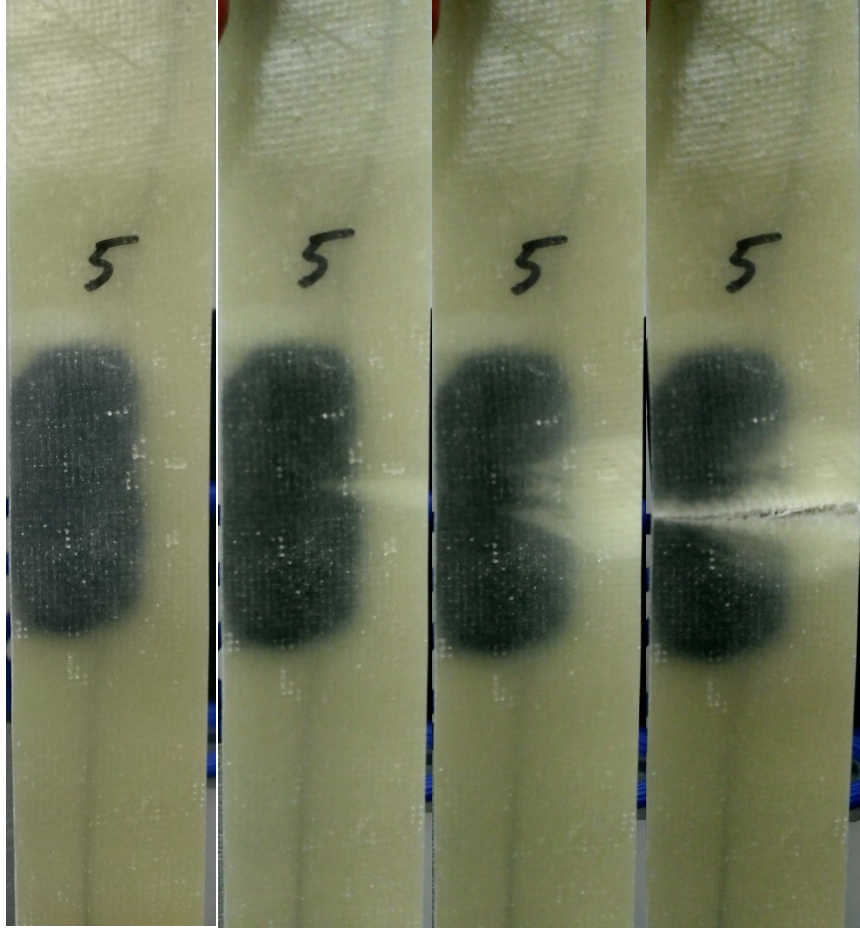


Figure 15. Delamination of sample 5 containing CNTs as loading is increased (left to right)



Figure 16. Side view of CNT sample 5 showing small delamination in composite

Table 4 shows the % difference from the bare aluminum to both the composite samples and the CNT samples. The composite samples show an increase in max loading of 152.62% while the CNT shows 102.14%. Both are over double the loading as

compared to the bare aluminum which describes that the added composite increases the strength of the aluminum. The only difference between the CNT samples and the composite samples is the addition of the CNTs but a significant decrease in maximum loading is observed as shown in Table 4. One method utilized to explain the difference included looking at the difference in thickness between the two sets of samples. The samples with CNTs have an increased thickness at the section from the crack tip to the edge of the samples while there is no increase in thickness at the cracked section. In other words, the increased thickness in the location of loading was resulted from inclusion of the CNTs at the location. Table 5 shows the difference in thickness from the composite samples to the CNT samples on the loading side.

Table 4. Breakdown comparison of loading for each set of samples

	Average	SD	% Difference from Bare	%Difference from Composite
Bare	6,005.84	132.04	0.00	N/A
Composite	15,172.18	309.58	152.62	0.00
CNT	12,140.23	1,258.68	102.14	-19.98

Table 5. Thickness of composite and CNT samples

	Composite thickness (mm)	CNT thickness (mm)
Sample 1	4.60	5.65
Sample 2	4.60	6.55
Sample 3	4.00	6.80
Sample 4	4.65	6.85
Sample 5	4.70	6.00
Average	4.51	6.37
SD	0.24	0.43

Table 5 demonstrates that the thickness of the CNT samples averages almost 2mm thicker. In real shipboard fleet application the aluminum will be thicker and thus the composite patch will be thicker as well. The size of the CNT sensor will not change no

matter how many plies are added for the composites final thickness. This will decrease the overall difference in thickness between the composite alone as compared with the addition of the CNTs. The current large difference in thickness in a local area will change the maximum stress observed within the samples. Figures 17 and 18 show the deformation of two samples modeled in ANSYS. Figure 17 shows the model with CNTs added as a block on top of the composite, where Figure 18 shows the model with only the composite. Though not physically exact in appearance, the model does show the correct qualitative results. Comparing Figures 17 and 18, the deformation for the sample with CNTs is larger than that without the CNT's. The higher deformation corresponds to a larger stress and thus supports the testing as the higher stress would cause the CNT samples to fail at a lower load.

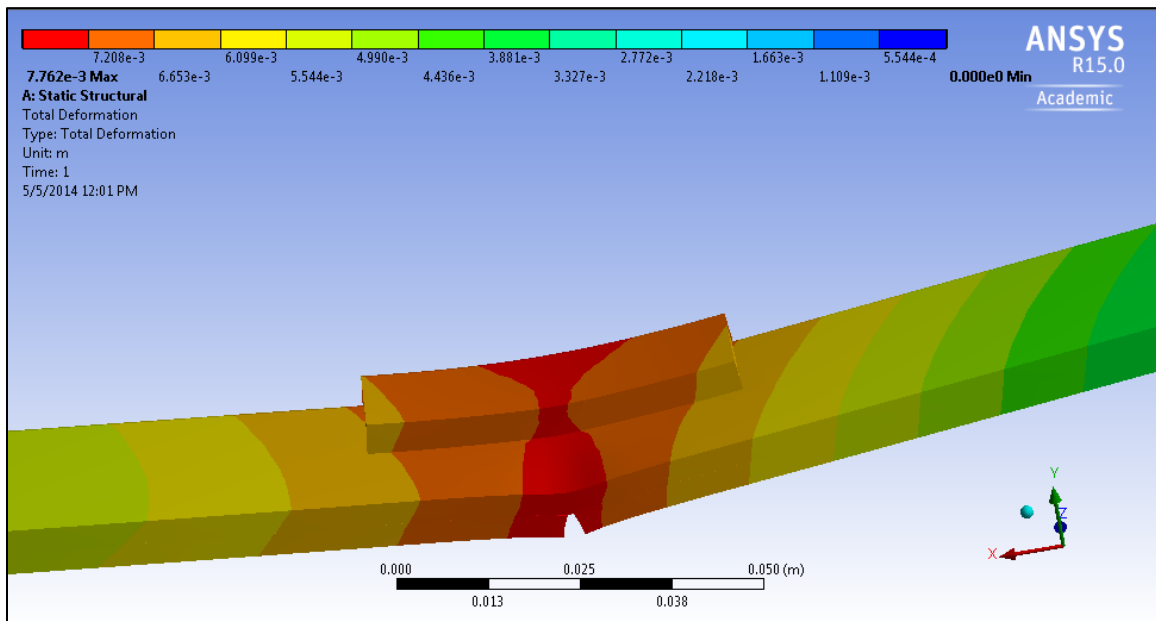


Figure 17. Deforpmation for composite sample with CNT's on top as top square

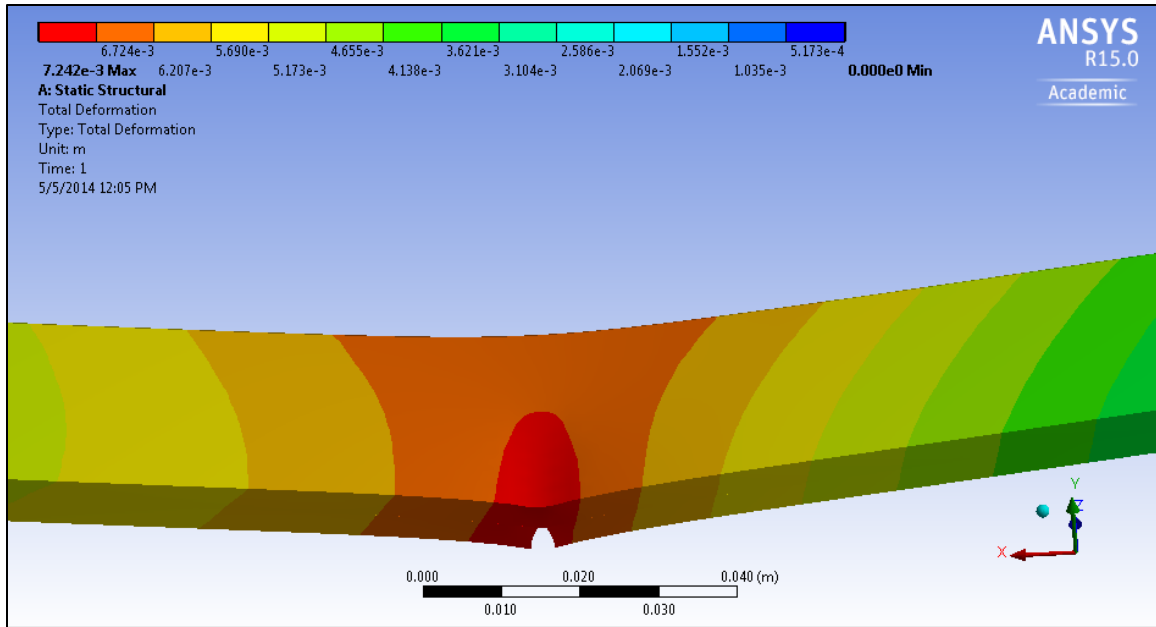


Figure 18. Deformation for composite sample

Figure 19 shows the initial and final resistance for each CNT sample. It is shown graphically in Figure 19 and numerically in Table 6 that the resistance increases greatly as compared to its initial resistance. The crack propagation was measured at the end of testing and was compared to the change in resistance to give a change in resistance per crack length growth shown in Table 6.

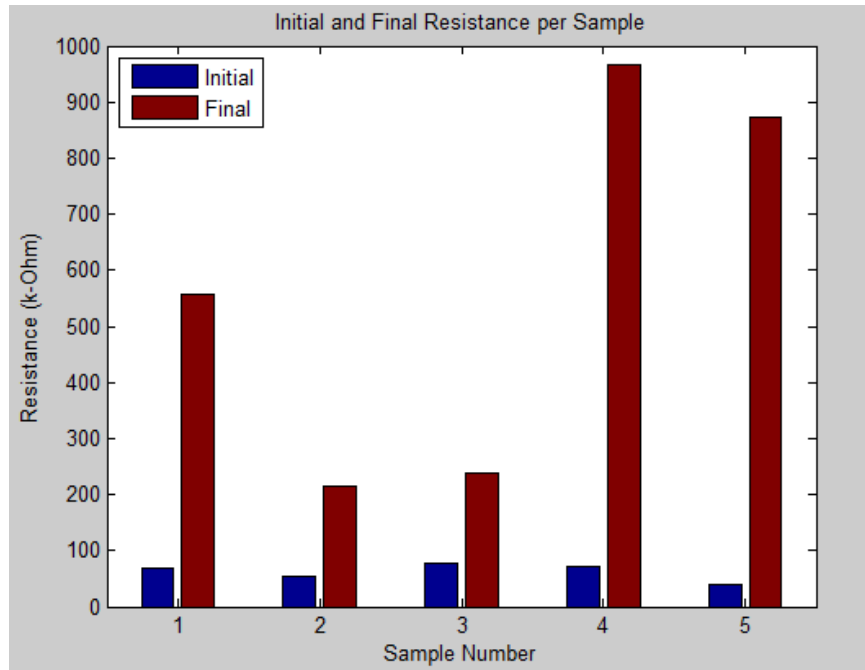


Figure 19. Tensile loading resistance graph

Table 6. Resistance increase per crack length

	Change in resistance (kΩ)	Crack propagation length (mm)	Change in resistance per crack length (kΩ/mm)
Sample 1	487.63	5.20	93.77
Sample 2	259.98	5.10	50.98
Sample 3	160.60	5.35	30.02
Sample 4	894.97	7.75	115.48
Sample 5	833.66	7.80	106.88
Average	527.37	6.24	79.43
SD	269.74	1.15	30.30

B. FATIGUE TESTING

Similar to the tensile testing, all fatigue testing was based on five samples of same design and composition. Three sets of samples (bare aluminum, composite, composite with CNT sensor) were created in order to show the difference between each. All samples were cycled +/- 1 kN from a mean of 4 kN at a frequency of 10 Hz. Initial testing with mean loading much larger than 4 kN resulted in rapid failure. Testing with

mean loading lower than 4 kN resulted in a high cycle life prior to failure around 1 million cycles. In order to decrease time to failure for a sample but to still show a reasonable number of cycles, a mean of 4 kN was chosen.

1. Bare Aluminum

From the tensile testing, it was shown that the bare aluminum failed around 6 kN. It is commonly understood that materials fail at much lower loads under cyclic loading than straight tensile loading. Thus, cycling the bare aluminum at a load near its maximum tensile load resulted in a rapid failure with very few cycles. It is still important to have this data though as it is a baseline comparison for the composite and CNT samples. Table 7 shows the cycles to failure for each sample. Figure 20 shows a view of the crack after fracture. The fracture surface is sharp and at a 45 degree angle, thus showing ductile failure of the aluminum. This type of failure occurred as crack propagated rapidly.

Table 7. Bare aluminum cycles to failure

Cycles	
Sample 1	59
Sample 2	67
Sample 3	68
Sample 4	65
Sample 5	58
Average	63
SD	4

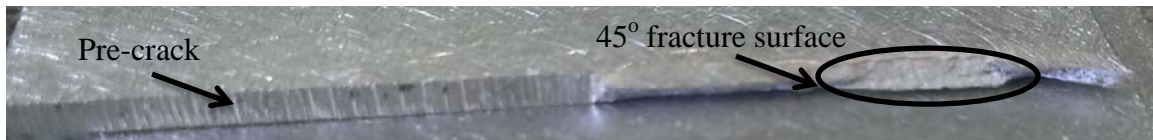


Figure 20. End view of bare aluminum showing fracture surface

2. Composite

As assumed and desired, the composite strengthened the aluminum preventing it from failing rapidly as compared to the aluminum alone. The number to cycles to failure

in the aluminum is shown in Table 8. There appears to be a lot of variance in the data as the standard deviation is almost 67,000 cycles but even the lowest number of cycles to failure is over 100,000% higher than that of bare aluminum. Figure 21 shows the delamination occurring during the cyclic loading for sample 1 of 5 samples.

Table 8. Composite cycles to failure

Cycles	
Sample 1	528,292
Sample 2	580,209
Sample 3	479,147
Sample 4	415,238
Sample 5	623,143
Average	525,205
SD	66,884

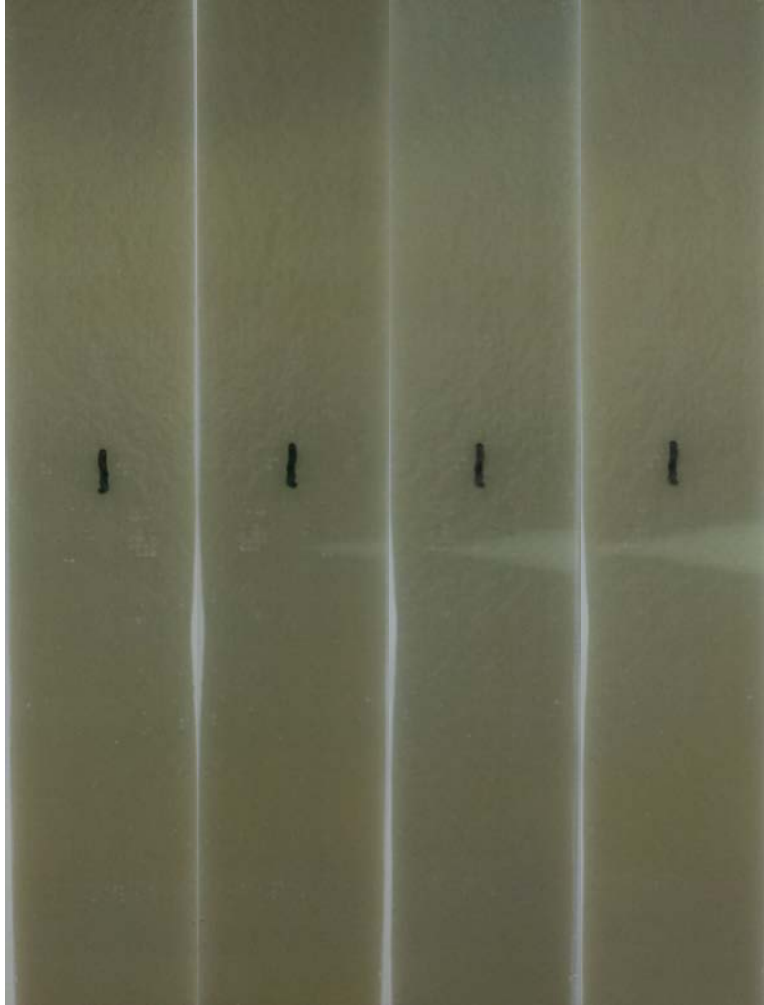


Figure 21. Delamination of sample 1 during loading from no load (left) to aluminum has fully fractured (right)

Figures 22 and 23 are side views of sample 4 showing that the delamination is only in the composite. There is no delamination between the aluminum and the base layer of resin or between the base layer and the composite. Figure 23 shows an intact bond between the aluminum and the base layer and it is visible that there is no cracking of the base layer as compared to and shown in the tension samples.



Figure 22. Sample 4 showing delamination within the composite only



Figure 23. Sample 4 showing no delamination between layers or aluminum

Figure 24 shows the growth of the crack during cyclic testing of sample 1. Comparing figures 10 and 24, less delamination occurred with the cyclic testing and the aluminum completely failed while the composite remained intact. The tension testing showed the composite would fail before the aluminum. For cyclic testing the opposite occurred. Figure 25 shows the cracked edge of sample 2 and it is apparent the fracture surface shows brittle fracture. At high cycles it is common for materials that normally fail showing ductile fracture to fail showing brittle fracture. Under cyclic loading the composite did not fail but the aluminum did. In order to show the fracture surface of the aluminum, sample 2 was tensioned to cause failure in the composite.

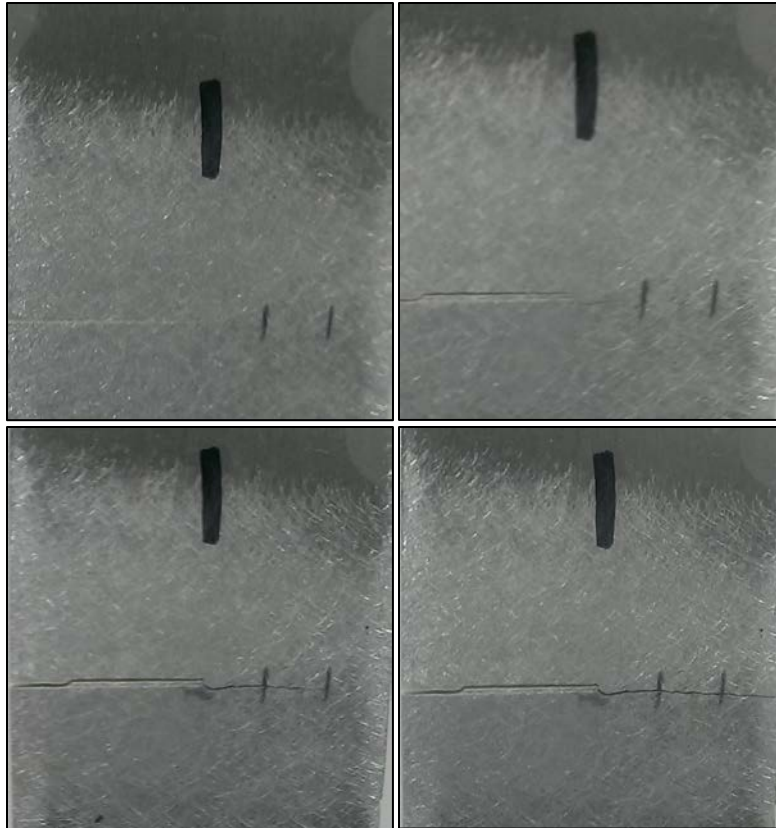


Figure 24. Growth of crack in aluminum for composite sample 1 from no cycles (top left) to under $\frac{1}{4}$ inch (top right) to $\frac{1}{2}$ inch (bottom left) to complete failure (bottom right)



Figure 25. Cracked edge of sample 2 showing brittle fracture surface

3. Composite with CNT Sensor

Similar to the tension testing the only difference between the composite samples and the CNT samples is the addition of the CNTs. Table 9 shows the cycles to failure for the CNT samples. The smallest cycle to failure is over 100,000% above bare aluminum cycles to failure. Though on average fewer cycles were needed to propagate the crack in the aluminum the composite with CNT did not fail showing consistency. Figure 26 shows the delamination in CNT sample 2 while the crack was growing. The amount of delamination in the CNT samples as compared to the composite samples is very similar. This shows consistency in sample failure between the CNT and composite samples.

Table 9. CNT cycles to failure

Cycles	
Sample 1	137,473
Sample 2	351,160
Sample 3	274,062
Sample 4	194,043
Sample 5	229,158
Average	237,179
SD	72,413

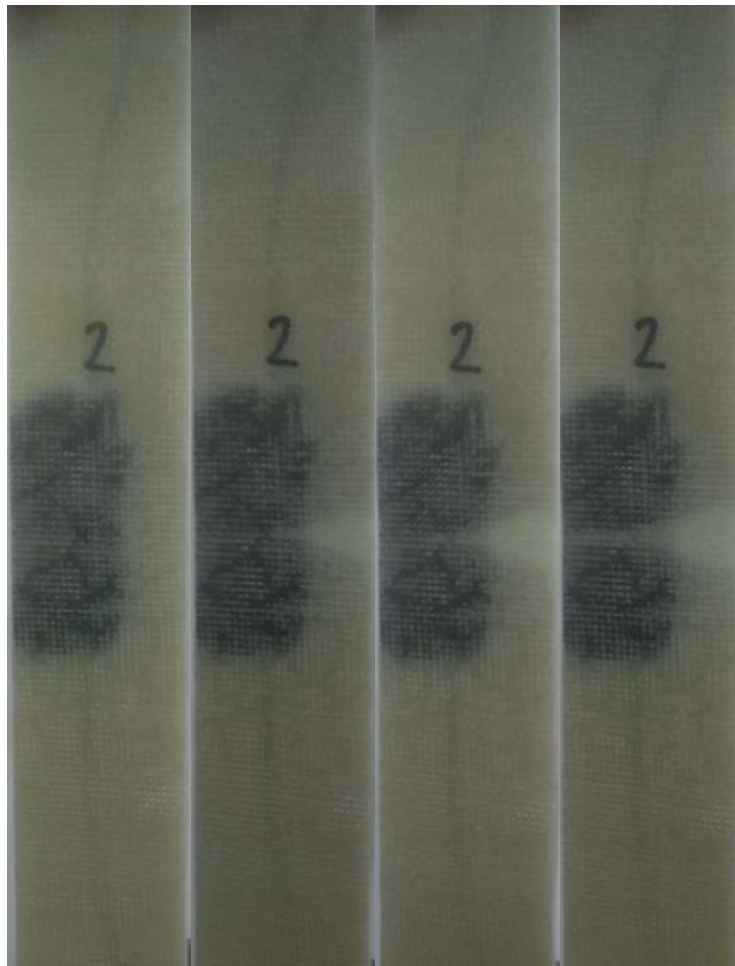


Figure 26. Delamination of sample 2 during loading from no load (left) to aluminum almost fully fractured (right)

Figure 27 shows the delamination only occurring in the composite which is the same seen in the composite samples. Figure 28 shows no delamination occurring

between the aluminum and the base resin layer or the base resin layer and the composite. This is also consistent with the composite samples which reduce probability of errors in sample preparation.



Figure 27. Sample 2 showing delamination within the composite only



Figure 28. Sample 2 showing no delamination between layers or aluminum

Figure 29 shows the crack growth from no loading to complete failure of the aluminum. The crack growth in the CNT samples is also consistent with the composite samples. The fracture surface is also consistent with the composite samples as brittle fracture can be observed in Figure 30. Similar to the composite, CNT sample 2 was placed under tension after failure of the aluminum in order to cause the composite to fail and inspect the fracture surface. This shows the failure mechanism is the same for both the composite and CNT samples. Having the same failure mechanism for both sets of samples reduces the probability that the added CNTs are having a negative effect to the overall sample strength.

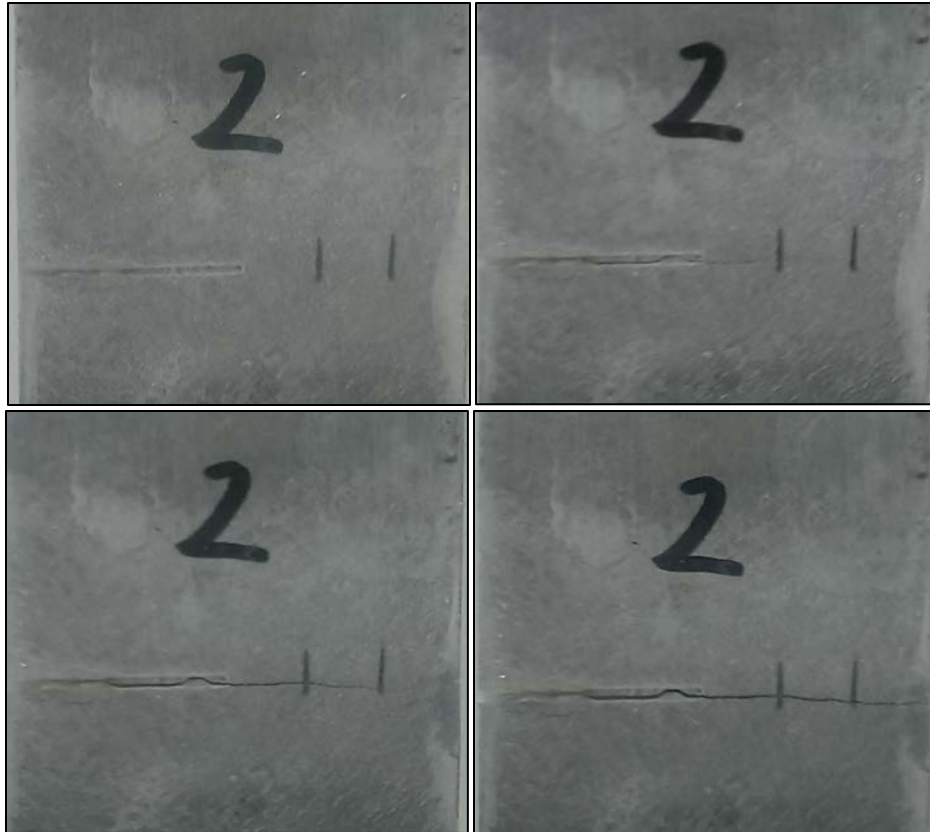


Figure 29. Growth of crack in aluminum for CNT sample 2 from no cycles (top left) to under $\frac{1}{4}$ inch (top right) to $\frac{1}{2}$ inch (bottom left) to complete failure (bottom right)

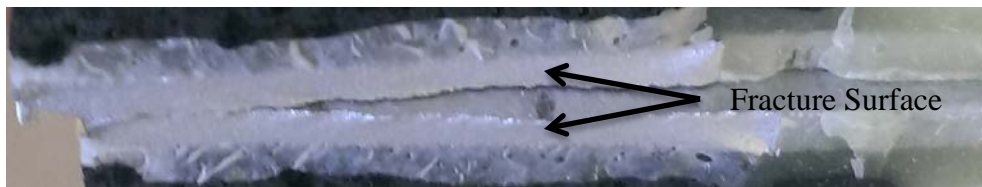


Figure 30. Cracked edge of sample 2 showing brittle fracture surface

Table 10 shows the comparison between the different samples and their number of cycles to failure in the aluminum. It is apparent that both the composite and CNT samples drastically increase the average cycles to failure by over 3,000 times, but it is also apparent that the composite and CNT samples are different. This can be attributed to the same reasoning behind the difference in the tension testing. From ANSYS modeling shown in the tension tests it can be seen that the deformation in the CNT is higher in

some areas than the composite thus causing the sample to fail at a lower load. Similarly, failing at a lower load would show in fatigue as a decreased number of cycles to failure as shown numerically in Table 10 and graphically in Figure 31. The error bars shown in Figure 31 represent the SD for each set of samples. The y axis is log scale in order to see the bare aluminum cycles as the composite and CNT cycles are so much larger.

Table 10. Numerical comparison between bare aluminum, composite and CNT cycles to failure

	Average	SD	% Difference from Bare	%Difference from Composite
Bare	63	4	0.00	N/A
Composite	525,205	66,884	828,300	0.00
CNT	237,179	72,413	373,999	-54.84

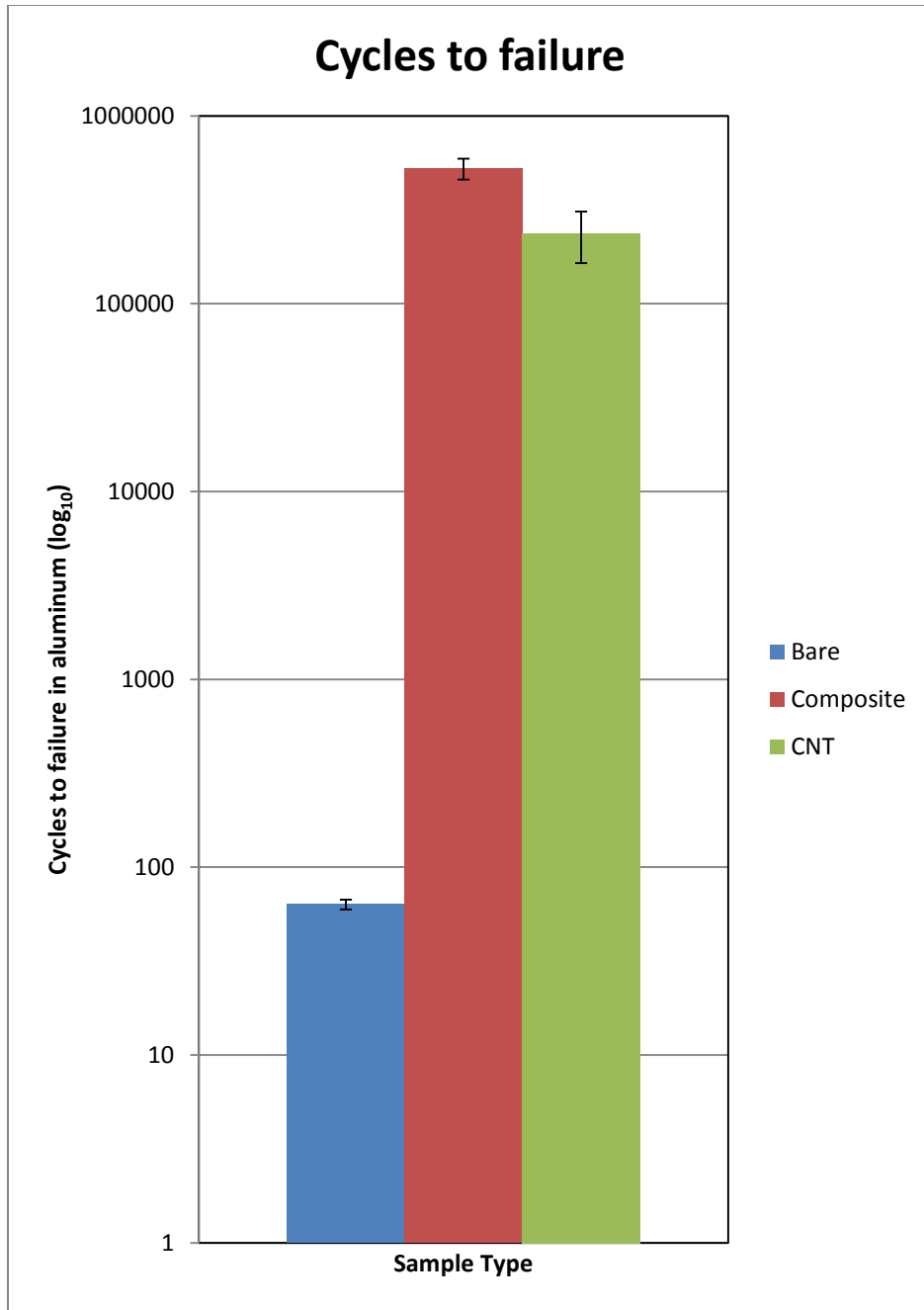


Figure 31. Graphical comparison between bare aluminum, composite and CNT cycles to failure

Figure 32 shows the resistance change during cycling up to complete failure of the aluminum. The error bars shown are $\pm 1\text{k}\Omega$ as there was a variance in the recorded resistance during monitoring. To increase accuracy the resistance was measured continuously. It is apparent that the resistance always increases as the crack grows but in

some cases it is not a large change. It is important to note after the aluminum failed the resistance did not change greatly and the crack or separation of the aluminum was not very large as it was on around 0.05 mm. For the resistance to change more the crack must be larger. Furthermore, upon unloading the sample the resistance typically decreased back down to around the resistance recorded at the 1/2 inch location. This is also important as the resistance change must be large enough to notice an appreciable change in order to not have a false reading where someone would think the crack is growing when it is not.

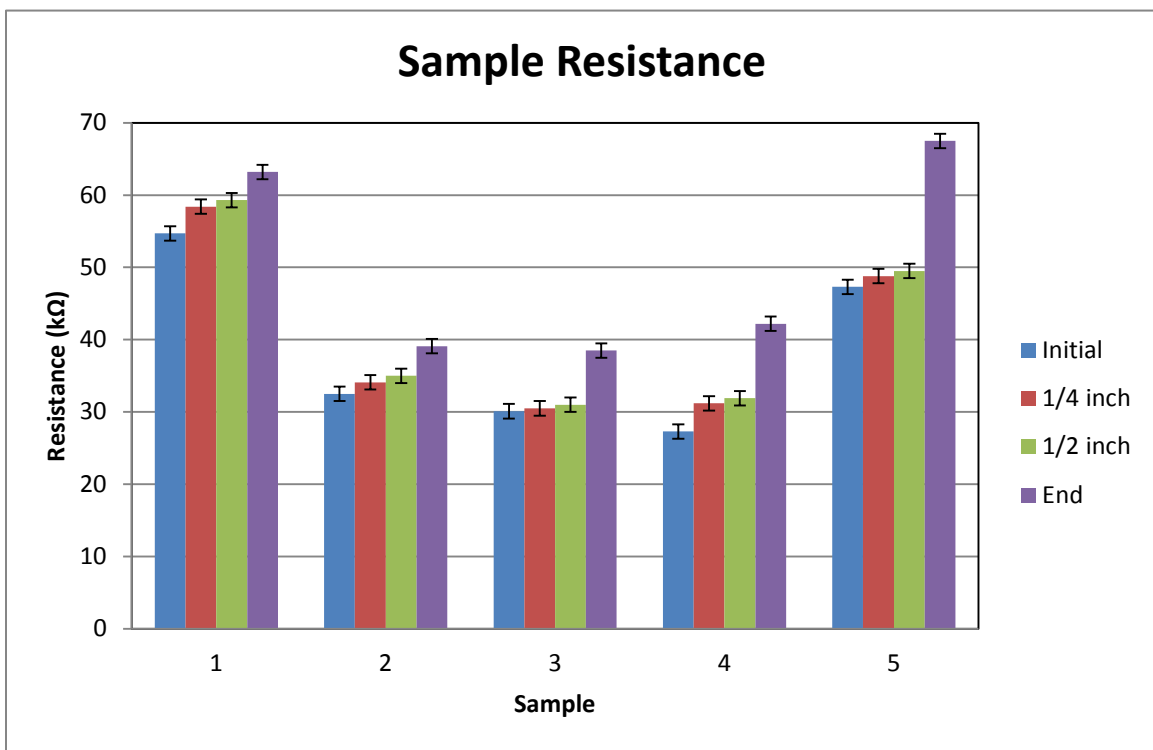


Figure 32. Cyclic fatigue resistance change for each sample

THIS PAGE INTENTIONALLY LEFT BLANK

IV. CONCLUSION

All objectives were met as a CNT sensor was created and fabricated into samples. Those samples were then tested in both tensile and cyclic loading. The CNT sensor proved to work dependent on delamination and overall resistance described below.

A. DELAMINATION

Utilizing the current bonding agent prevented delamination from occurring between the aluminum and the base layer of resin and from the base layer and the composite. Some delamination occurred on the top and bottom of the tensile samples but it did not occur in the fatigue samples. Delamination was seen mainly in the composite itself in both tensile and fatigue testing. In both cases the amount of delamination was similar. The delamination shown will typically not be visible in shipboard application as paint will be placed over the composite. Only delamination around the edges of the composite is typically visible.

B. RESISTANCE

In both tests resistance increased as the crack propagated. Though the tensile samples showed a greater increase in resistance, the explanation is based on the crack width and not necessarily length. All of the tensile samples had a crack width around 1.3 mm where the fatigue samples were around 0.7 mm. The increased crack width in the tensile samples allowed for a larger crack in the CNT which caused a larger change in resistance. It was observed that once the loading was removed after failure of the aluminum in the fatigue testes the resistance decreased back near the resistance recorded when the crack was ½ inch in length. This decrease in resistance increases the difficulty in reading the resistance of the sensor accurately as in shipboard application it will be unknown if the location is under tension or at rest.

C. USEFULNESS

It is clear from this study that CNTs can be utilized as a sensor to detect growth of a crack in aluminum structures. The amount of CNT added to the resin needs to be

around 5 wt% as it decreases the initial resistance low enough to be able to detect a change during crack growth. It is shown in this study that though there was an increase in resistance in each sample for fatigue testing, the increase is not large enough to be detected accurately without having constant monitoring. Thus, the crack would grow past the sensor to an unknown value in length until the crack width would be large enough to have an effect to the CNT sensor. It is uncertain and more testing needs to be completed on larger samples in order to determine how long the crack must grow to have an appreciable increase in resistance under fatigue testing. Though, at a minimum if the crack grows long enough to crack the CNT sensor completely the resistance would show zero which would still give indication that the crack has grown and the composite patch could be replaced. The process of creating the sensor and applying it to tip of the crack is easy enough that it could be turned over to ships force to complete after some training. This sensor would remove the unknown factor of whether the crack was growing or not.

APPENDIX A

A. INITIAL SAMPLE PREPARATION

Initially the samples were cut out of the sheet with a width of 1 and ½ inches and a length of 8 inches. The samples were prepared by creating the initial crack or v-notch as seen in Figure 33. This v-notch was used to give a higher stress concentration at the tip in order to initiate a crack at that location. This v-notch is more consistent to testing done by any American Society of Testing and Materials (ASTM) standard and allowed the study to closely follow the standard. The location and depth allows ease of placement for the CNT sensor within the direct path of the crack propagation. The notch created was ¼th of an inch to allow a reasonable distance for the crack to propagate after initiation.

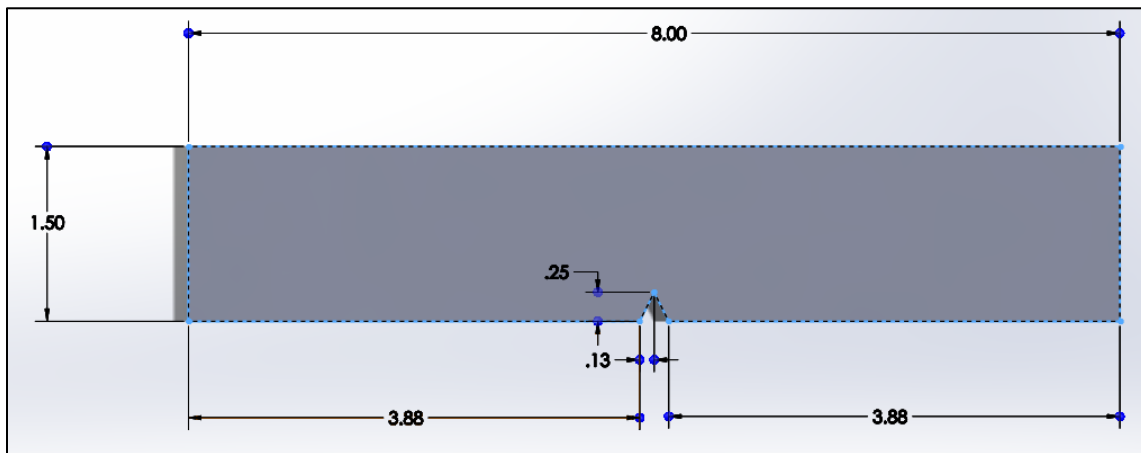


Figure 33. Diagram with measurements of initial sample design with notch, measurements are in inches

B. MATERIALS/EQUIPMENT

Most materials and equipment utilized initially are the same as the final design but those changed include:

- Size of aluminum sample (eight inches)
- Notch cut into sample
- (3-Glycidoxypropyl)-Trimethoxysilane (Saline bonding agent)
- Isopropyl Alcohol (for bonding agent)

- Oven (to bake bonding agent onto sample)

C. CONSTRUCTION TECHNIQUE/PROCEDURE

1. Initial

The construction procedure for an individual sample is show listed in order of completion. The specific materials utilized are outlined in the materials and equipment section.

a. Aluminum

- Cut out sample size to desired width and length (1 and ½ inches by 8 inches).
- Cut notch into sample to introduce stress concentration.
- Sand top side of sample to ensure entire surface is roughened.
- Clean metal surface with metal cleaning agent.

b. Bonding Agent

- Mix saline bonding agent with isopropyl alcohol and water, allow to sit for 30 minutes.
- Allow surface to dry from cleaning agent and apply water drop test. If test fails, repeat cleaning and test again.
- Apply saline bonding agent to surface and let sit for at least 1 minute.
- Remove excess saline bonding agent by dabbing a pre-wetted cloth with bonding agent. DO NOT RUB as described in directions on bottle for use.
- Place sample within oven and bake at 110 °C for one hour.
- Once baking is complete, remove sample and prepare resin.

c. Resin

- Mix resin and hardener as prescribed with thickener.
- Cover sample with a thin layer of resin and ensure notch is filled in. Let completely harden.
- Once hard sand top of sample to remove uneven locations and roughen the surface.

- Clean surface from sanded particles and dust.

d. CNTs

- Mix resin and hardener for CNT sensor.
- Weigh mixed resin and add four wt% of CNT to resin.
- Place CNT resin on sample in front of notch point.
- Place wire in both ends of the CNT resin long enough to extend past the end of the sample.
- Let CNT resin harden.
- Once hardened, sand top of CNT resin to roughen the surface.
- Clean surface from sanded particles and dust. (Test initial resistance)

e. E-Glass

- Cut set number of e-glass fibers to needed size and shape.
- Mix resin and hardener for composite.

f. Create Composite

- Apply e-glass fiber sheets and coat with resin ensuring even and full coating.
- Apply bleeder sheet to top of sample followed by cloth.

g. Vacuum Seal Composite

- Place seal over entire sample and vacuum out air to -10 mmHg and hold for eight hours.
- Once hardened remove excess epoxy and test sample.

2. Final Changes

Changes were made from this initial sample preparation to the final one shown in the Experimental section and the reasoning behind each change is described.

a. Sample Size

The initial sample size of 8 inches was selected due to the initial settings of the instruments being utilized including the MTS. After initial testing, shown in Appendix

B, it was determined that the length needed to be increased to allow a larger bonding area to prevent delamination between the composite and the aluminum. Delamination is a possible outcome in the composites placed on ships, but not catastrophic delamination as was seen in the testing. Also, a larger composite area more closely reflects the relationship of the composites placed on ships and the results more closely reflect what is being seen in the fleet.

b. Notch

Initially a notch of $\frac{1}{4}$ inch in length was employed. After initial testing it was determined in order to avoid delamination, the load required to initiate the crack needed to be lower than the load which caused delamination. To decrease the load to initiate the crack, the initial crack length was increased to $\frac{3}{4}$ th of an inch. This distance is half of the overall width of the sample. It ensures the loading is transferred from the aluminum to the composite at a load below the minimum required for delamination.

c. Bonding Agent

Initially (3-Glycidoxypropyl)-Trimethoxysilane was used as the bonding agent. It is considered a saline agent, meaning it consists of liquid. It was the bonding agent initially used by the fleet for composite applications on ships and it was readily available in the laboratory. This specific bonding agent requires a mixture of it with isopropyl alcohol and water. By volume, the mixture was 95ml isopropyl alcohol, 5ml water and 5 ml of the bonding agent. It was to be mixed and let sit for 30 minutes similar to the final 3M bonding agent utilized which is also a saline agent. The application process was also the same, but it was then required to be baked in an oven at 110°C for one hour. This process is not completely feasible to complete in situ on a ship. Also, upon testing the bonding agent did not hold as efficiently shown in Appendix B. The bonding agent was changed to the same currently being utilized in the fleet. It is still a saline bonding agent, but does not require baking the sample (impractical if attached to a ship) and has observable better bonding characteristics. No official information was found for either material in order to compare bond strength, but through testing it was observed that de-

bonding occurred when the initial bonding agent was utilized while the newer bonding agent had little to no de-bonding.

d. Curing Time

Initially, after creating and applying each resin set, the resin was allowed to fully cure and harden. It was then sanded and the next part was completed and placed on top. From testing shown in Appendix B delamination occurred between the composite and the base resin layer. The bond between the two hardened resin layers was not strong enough to prevent delamination. The final construction procedure is based on curing time and not allowing the resin to fully harden before applying the next part. The tackiness of the resin creates a stronger bond then applying new resin to completely hardened resin.

THIS PAGE INTENTIONALLY LEFT BLANK

APPENDIX B

A. INITIAL TESTING

1. Eight-Inch Samples

Larger widths of aluminum were utilized during initial bare aluminum testing. As seen in Figure 34 warping occurred on the left side due to the sample being in compression. This was an undesirable outcome which did not match any fleet responses, and thus the sample width was decreased to 1 and ½ inches.



Figure 34. Bare aluminum sample with 3-inch width, warping can be seen on left side

With the correct width established, testing was completed to determine if the sensor would initially work without the composite on top on the aluminum covering the crack. Figure 35 shows the cracking aluminum underneath the cracked CNT sensor. This test proved that as the sensor cracked the resistance rose which is consistent with previous studies and the resistance increase could be correlated to an increase in crack

length in the aluminum. It could be seen though at this initial stage, delamination occurred underneath the CNT sensor between the initial resin layer and the aluminum. This would be later contributed to the bonding agent and the overall curing time process as seen in Figure 36.



Figure 35. CNT sensor utilization and proof of usability

Initial composite testing utilized eight inch notch samples, with the (3-Glycidoxypropyl)-Trimethoxysilane bonding agent, and allowed full curing between each layer. Figure 36 shows delamination which occurred during tension testing. Delamination started at the ends and under the notch location in the center of the sample. Eventually catastrophic delamination occurred on the entire upper side (top of Figure 36) of the sample. Catastrophic delamination is described as extremely rapid delamination which typically occurs within one second. All samples were only tension tested initially

to ensure repeatability of design and process. Cyclic testing was completed later utilizing the final procedure and materials.

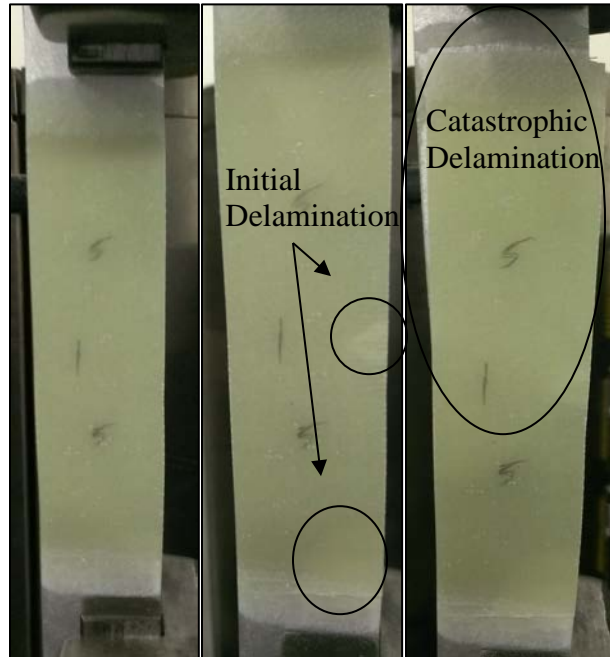


Figure 36. Eight inch samples, before testing (left), initial delamination (middle), final catastrophic delamination (right)

As seen in Figure 37, delamination occurred between the base resin layer and the composite on top. This was due to allowing the base layer to fully cure before applying the composite.

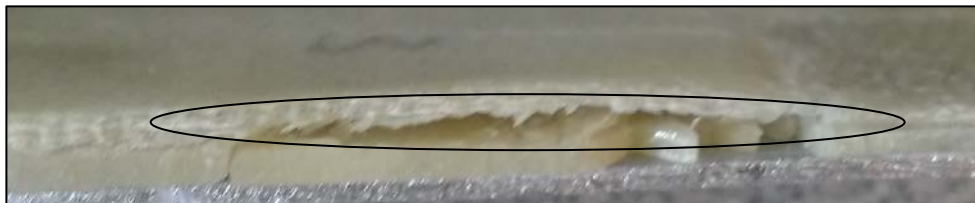


Figure 37. Delamination occurring between the base resin layer and the composite

The design of the composite allowed for 1 inch of bare aluminum at each end for the testing machines to grip the sample. In true shipboard fleet applications the loading

will pass from the base aluminum to the composite. The forces applied will not completely load the composite by itself, thus it was important not to place the loading in this study directly onto the composite. Upon testing results where 13 out of 15 samples showed major delamination, the composite was altered to be the full length of the aluminum. This would change the loading in the composite where it would now take all of the loading which is not consistent with fleet application but was tried in order to solve the delamination issue. Figure 38 shows a full length composite sample from no loading to near complete failure of the sample. The white looking area is delamination between the composite and the base resin layer. In this set of samples the delamination occurred most between the base resin layer and the composite. There was little to no delamination between the aluminum and the base resin layer as seen in Figure 39.



Figure 38. Full length composite sample, initially unloaded (left), initial delamination (middle), final delamination (right)



Figure 39. Full length composite sample showing delamination between the base resin layer and the composite

Finally, testing was completed utilizing the CNT sensor as shown in Figure 40. It can be seen that delamination occurred on the right side of the sample as the slight white part shows the delamination between the aluminum and the base resin layer, also seen in a side view in Figure 41. The brighter white locations near the bottom shows delamination between the composite and the base resin layer. Due to the delamination between the base resin layer and the aluminum the CNT sensor proved ineffective. It was concluded that in order for the sensor to work there could be little to no delamination between the base resin layer and the aluminum, and between the CNT sensor and the base layer of resin.

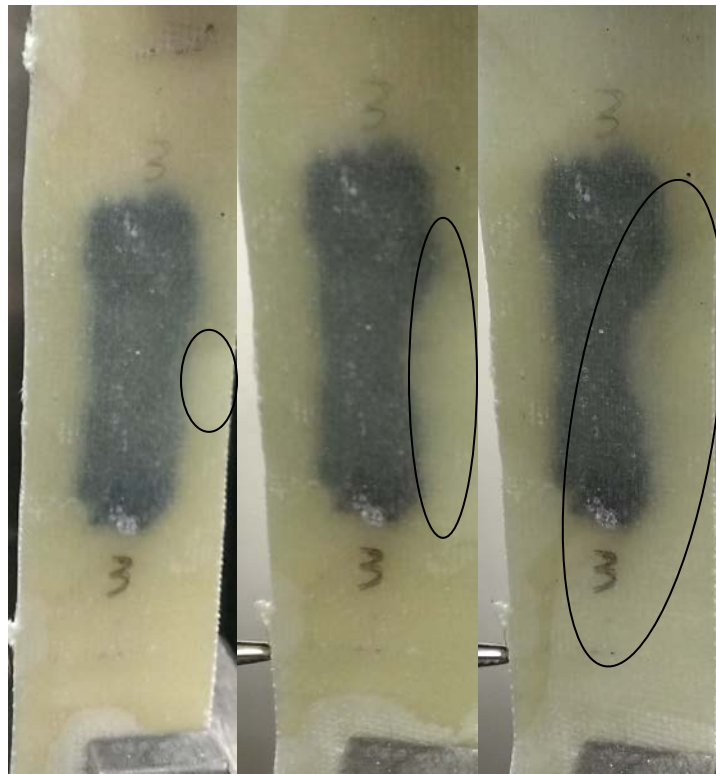


Figure 40. Full length composite sample with CNT sensor, initially unloaded (left), initial delamination (middle), final delamination (right)

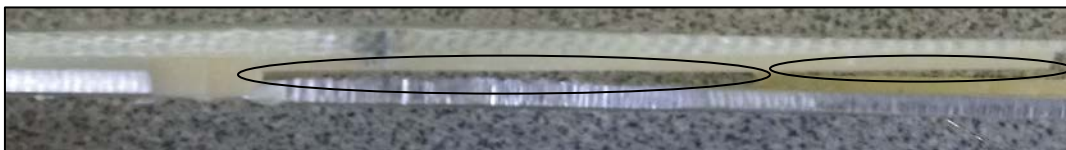


Figure 41. Full length composite with CNT sensor showing delamination between both base resin layer and aluminum (middle) and base resin layer and composite (right)

2. Twelve-Inch Samples

Based on the previous eight inch sample testing, the length of the samples were increased to 12 inches. This gives 10 full inches of composite and allows one inch of exposed aluminum at each end for the test equipment to grip the sample, thus keeping to actual shipboard loading. Initial testing utilizing 12 inch samples showed favorable results as shown in Figure 42. The crack propagated in the aluminum. There was much less delamination and it was only in the area of the crack propagation. The delamination as seen from the side in Figure 43 was between the base layer of resin and the composite.

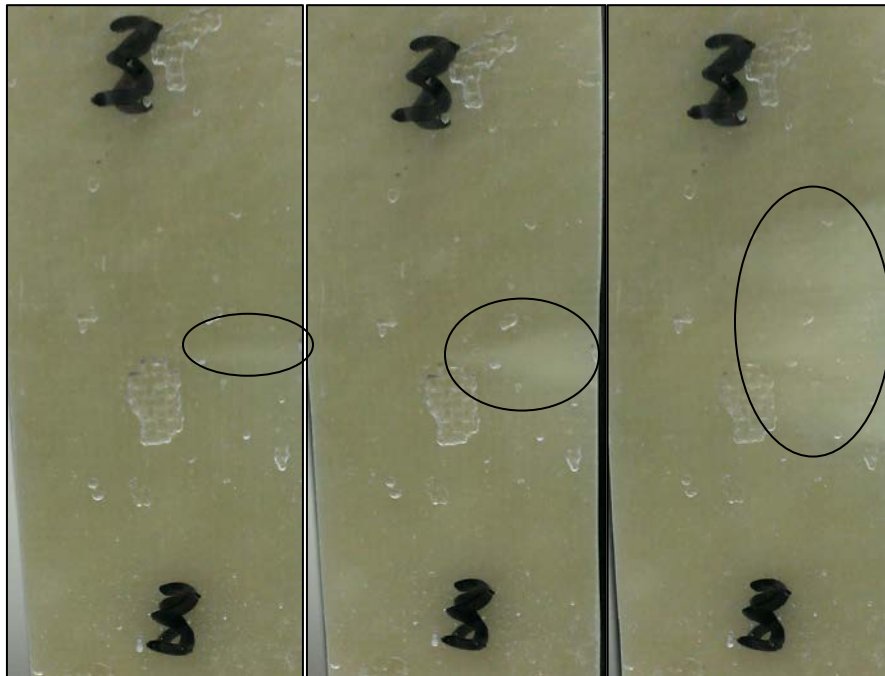


Figure 42. 12 inch sample showing delamination progression around pre crack area from left to right

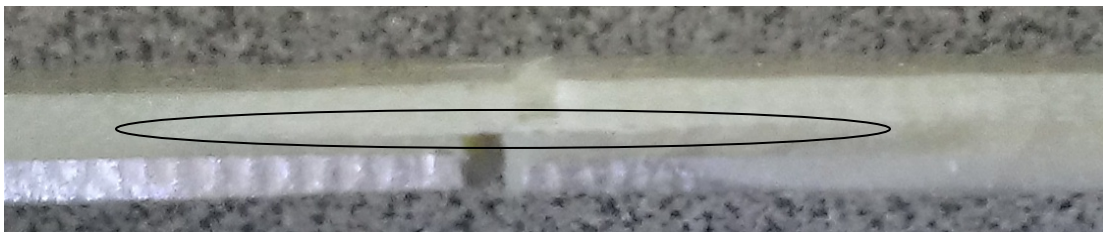


Figure 43. Delamination between the base resin layer and the composite around the crack area

From this testing it was concluded that the 12 inch sample size was the correct size and that by changing the bonding agent and the method of allowing the base resin layer to fully cure would improve the results to be comparable to that seen in actual shipboard application. This would allow for the CNT sensor to function as designed and would work with any base material, not just aluminum. Further testing was completed using the updated procedure and changed materials and are shown in the experimental and results sections of this study.

THIS PAGE INTENTIONALLY LEFT BLANK

LIST OF REFERENCES

- [1] R. Schwarting, G. Ebel and T. Dorsch, "Manufacturing techniques and process challenges with CG47 class ship aluminum superstructures modernization and repairs," in *In Fleet Maintenance and Modernization Symposium 2001: Assessing Current and Future Maintenance Strategies*, San Diego, CA, 2011.
- [2] B. Needham and A. Field, "Sensitization of 5000 Series Al Alloys," presented at the Mega Rust conference, San Diego, CA, June 3–8, 2007.
- [3] A. Mouritz, E. Gellert, P. Burchill and K. Challis, "Review of advance composite structures for naval ships and submarines," *Composite Structures*, vol. 53, pp. 21–44, 2001.
- [4] W. D. Calister, "Carbon nanotubes," in *Materials and Engineering An Introduction*, New York, John Wiley and Sons, 2010, p. 471.
- [5] Ahwahnee, "Technical report: How to use multi-walled carbon nanotubes," Ahwahnee Technology Inc., San Jose, CA, ATI-2005-04, Rev. 1b, Oct. 12, 2005.
- [6] F. H. Gojiny, M. H. G. Wichmann, U. Kopke, B. Fiedler and K. Schulte, "Carbon nanotube-reinforced epoxy-compo sites: enhanced stiffness and fracture toughness at low nanotube content," *Composites Science Technology*, vol. 64, no. 15 pp. 2363–2371, 2004.
- [7] M. Bily, "Study of composite interface strength and crack growth monitoring using carbon nanotubes," M.S. Thesis, Naval Postgraduate School, Monterey, 2008.
- [8] R. Saito and G. Dresselhaus, "Physical properties of carbon nanotubes," *World Scientific*, pp. 11–12, 224–225, 1998.
- [9] The Venton Research Group, "Development of carbon nanotube modified microelectrodes" [Online]. Available: <http://www.faculty.virginia.edu/ventongroup/nanotube.html>.
- [10] S. Faulkner, *Study of composite joint strength with carbon nanotube reinforcement*, Monterey: M.S. Thesis, Naval Postgraduate School, 2008.
- [11] L. Gao, E. T. Thostenson, Z. Zhang, J. Byun and T. Chou, "Damage monitoring fiber-reinforced composites under fatigue loading using carbon nanotube networks," *Philosophical Magazine*, vol. 90, no. 31-32, pp. 4085–4099, 2010.
- [12] F. H. Gojny, M. H. G. Wichmann, B. Fiedler, I. A. Kinloch, W. Bauhofer, A. H. Windle and K. Schulte, "Evaluation and identification of electrical and thermal conduction mechanisms in carbon nonotube/epoxy composites," *Polymer*, vol. 47, no. 6, pp. 2036–2045, Mar. 2006.

- [13] E. T. Thostenson and T. Chou, "Real-time in situ sensing of damage evolution in advance fiber composites using carbon nanotube networks," *Nanotechnology*, vol. 19, no. 21, pp. 215–713, May 2008.
- [14] E. T. Thostenson and T. Chou, "Processing-structure-multi-functional property relationship in carbon nanotube/epoxy composites," *Carbon*, vol. 44, no. 14, pp. 3022–3029, Nov. 2006.
- [15] I. D. Rosca and S. V. Hoa, "Highly conductive multiwall carbon nanotube and epoxy composites produced by three-roll milling," *Carbon*, vol. 47, no. 8, pp. 1958–1968, July 2009.
- [16] L. Gao, T. Chou, E. T. Thostenson and Z. Zhang, "A comparative study of damage sensing in fiber composite using uniformly and non-uniformly dispersed carbon nanotubes," *Carbon*, vol. 48, no. 13, pp. 3788–3794, Nov. 2010.
- [17] E. T. Thostenson and T. Chou, "Carbon nanotube networks: Sensing of distributed strain and damage for life prediction and self healing," *Advanced Materials*, vol. 18, no. 21, pp. 2837–2841, Nov. 2006.
- [18] E. T. Thostenson, S. Ziaee and T. Chou, "Processing and electrical properties of carbon nanotube/vinly ester nanocomposites," *Composites Science Technology*, vol. 69, no. 6, pp. 801–804, May 2009.
- [19] J. Sandler, M. Shaffer, T. Prasse, W. Bauhofer, K. Schulte and A. Windle, "Development of a dispersion process for carbon nanotubes in an epoxy matrix and the resulting electrical properties," *Polymer*, vol. 40, no. 21, pp. 5967–5971, Oct. 1999.
- [20] W. Zhang, V. Sakalkar and N. Koratkar, "In situ health monitoring and repair in composites using carbon nanotube additives," *Applied Physics Letters*, vol. 91, no. 13, p. 133102, Sept. 2007.
- [21] C. Li, E. T. Thostenson and T. Chou, "Sensors and actuators based on carbon nanotubes and their composites: A review," *Composites Science Technology*, vol. 68, no. 6, pp. 1227–1249, May 2008.
- [22] B. Mahar, C. Laslau, R. Yip and Y. Sun, "Development of carbon nanotube-based sensor- A review," *IEEE Sensors Journal*, vol. 7, no. 1-2, pp. 266–284, Jan.–Feb., 2007.
- [23] M. Nofar, S. V. Hoa and M. D. Pugh, "Failure detection and monitoring in polymer matrix composites subject to static and dynamic loads using carbon nanotube networks," *Composites Science Technology*, vol. 69, no. 10, pp. 1599–1606, Aug. 2009.
- [24] Vishay Precision Group, "Micro-measurements, crack propagation patterns," [Online]. Available: <http://www.vishaypg.com/micro-measurements/>.

- [25] Pro-Set Inc., *Technical data, M1002 resin/237 hardener toughened laminating epoxy*, Bay City, MI: Pro-Set Inc., Aug. 2005.
- [26] Instron Corporation, *Test Method Development Manual*, Norwood, MA: Instron Corporation, 2004.
- [27] MTS Systems Corporation, *Controller Installation and Calibration*, Eden Prairie, MN: MTS Systems Corporation, 1999.
- [28] MTS Systems Corporation, *Model 793.00 System Software*, Eden Prairie, MN: MTS Systems Corporation, 2000.
- [29] U. S. Composites, "Fiberglass Cloth," 2011. [Online]. Available: www.uscomposites.com/cloth.htm

THIS PAGE INTENTIONALLY LEFT BLANK

INITIAL DISTRIBUTION LIST

1. Defense Technical Information Center
Ft. Belvoir, Virginia
2. Dudley Knox Library
Naval Postgraduate School
Monterey, California